

Mesure de l'angle de mélange θ_{13} avec les deux détecteurs de Double Chooz

Thèse de doctorat de l'Université Paris-Saclay
préparée à l'Université Paris-Sud

Ecole doctorale N°576 : PHENIICS
Spécialité de doctorat : Physique des particules

Thèse présentée et soutenue à Saclay le 16 novembre 2016 par

M. Valérian SIBILLE

Composition du jury:

M. Pierre DESESQUELLES

Professeur (CSNSM)

Président du jury

M. Fabrice PIQUEMAL

Directeur de recherches (CENBG)

Rapporteur

M. Michael WURM

Professeur (JGU)

Rapporteur

M. Thierry LASERRE

Ingénieur-Chercheur (CEA)

Examinateur

M^{me} Lindley WINSLOW

Professeur (MIT)

Examinateur

M. David LHUILLIER

Ingénieur-Chercheur (CEA)

Directeur de thèse

*An expert is a man who has made all the mistakes
which can be made in a very narrow field.*

Niels Bohr

Acknowledgements

L'épaisseur du manuscrit confère une certaine légitimité à l'auteur lorsque celui-ci entreprend l'écriture de remerciements tout aussi détaillés¹ que le contenu scientifique. Aussi vais-je en profiter et m'efforcer de ne laisser personne sur le bas-côté au cours de cette parade dithyrambique, tout en sachant qu'un *blitzkrieg* assure un déchargeement rapide du pavé dans les rayons de la bibliothèque universitaire, ultime consécration. Je m'excuse donc par avance auprès de tous les participants dont le lever de pouce fut trop discret pour que je fisse des embardées à leurs signaux non moins valables.

La sphère

Dans un premier temps, je remercie ceux sans lesquels rien de toute cette aventure n'aurait été possible, aussi limitées fussent nos interactions (on ne s'intéresse pas aux neutrinos pour rien) : Philippe CHOMAZ et son successeur à la tête de l'IRFU, Anne-isabelle ETIENVRE. Bien que soumises à une érosion perpétuelle, les conditions de travail en haut du plateau ne sont pas sans rappeler l'avantage qu'octroierait le dénivelé avec la vallée lors d'une bataille rangée. Dès lors, je souhaite remercier les chefs successifs du SPhN, Héloïse GOUTTE et Franck SABATIE, ainsi que le chef adjoint, Jacques BALL. Je tiens à m'attarder tout particulièrement sur le soutien de ces derniers lors des joutes finales qui nous ont opposés à la matouchka doctorale.

Le service du SPhN ne serait pas ce qu'il est sans Isabelle RICHARD, Danielle CORET et Valérie POYETON, que je remercie pour leur gentillesse, leur attention et leur efficacité ! Qu'il est agréable de pouvoir se défausser de certaines tâches sans être trop inquiet quant à l'issue ! Je remercie également Patrick CHAMPION d'avoir réparé, à plusieurs reprises, nos stores blancs transparents, dont le pouvoir d'arrêt contre les rayons lumineux, quoique faible, est décisif lors de la rédaction d'un manuscrit.

Le labeur

Au cœur de mon travail se trouve mon directeur de thèse, David LHUILLIER, auquel je témoigne toute ma reconnaissance pour la pertinence et la justesse de son encadrement. Ce physicien hors pair a su être derrière moi lorsque j'en avais besoin (alors que je ne m'en rendais pas toujours compte), notamment pour donner des limites et un cadre à l'exploration

¹La profusion de détails n'est pas un gage de qualité.

ACKNOWLEDGEMENTS

que constitue mon travail de thèse. Son approche directe et sa capacité à retranscrire des phénomènes physiques complexes, aussi aisément que pédagogiquement, ont opportunément perturbé mon équilibre chancelant. Bien que son temps libre fût victime d'un appauvrissement comparable à la décroissance d'un échantillon de ${}^9\text{Li}$, il s'est toujours jeté – feutre en main – sur les problèmes physiques que je pouvais lui poser, mettant parfois fin à plusieurs jours de questionnement en quelques minutes. En sus de ses qualités techniques indéniables, David est un directeur accommodant et compréhensif, soit tout bonnement humain.

Had it not been for these bloated acknowledgements, this document would have been entirely reviewed by Fabrice PIQUEMAL and Michael WURM; I thank them dearly for appreciating my peculiar writing style and fondness for rigorous descriptions! I thank them equally for coming from Bordeaux and Mainz, respectively, to attend my viva voce. I also owe Lindley WINSLOW for being available remotely at 4am (Boston time) whilst retaining enthusiasm, Thierry LASSEUR for travelling from Munich, and Pierre DESESQUELLES for presiding over the committee.

On revient toujours à l'un des pères fondateurs de Double Chooz, Thierry. Je lui suis reconnaissant de m'avoir poussé à travailler sur les mesures de pesée, sujet, comme il le souligne justement, fort simple sur le principe, mais autrement plus épineux lorsqu'il s'agit d'afficher des systématiques maîtrisées. Je lui sais gré de sa confiance, sa gratitude et son soutien pour l'obtention d'un post-doc, il n'est pas pour rien dans ce qui m'attend à Boston. Ces analyses de mesures de pesée ont été accompagnées d'un travail quasi-archéologique sur un tissu de données suranné; cette fouille au centre principal n'aurait jamais porté ses fruits sans la disponibilité de Jean-Christophe BARRIERE. Mentionner le centre conduit naturellement à remercier Guillaume MENTION, auquel je dois la relecture assidue de la note technique sur les simulations de spectres et des encouragements, qui ont assis la validité de mon entreprise. De la même manière, je ne saurais oublier cette semaine de calibration intense à Chooz, avec Matthieu VIVIER, agrémentée d'Ardennaises livrées par notre porte-parole, Hervé de KERRET, et consommées dans l'empressement. La parenthèse musicale dans la voiture, ainsi que les discussions sur le monde de la recherche, ont été autant de données pour mon étalonnage interne. Non sans poids dans le succès de cette thèse, je dois mon premier *shift* et mes premières incursions en territoire belge houblonné à Vincent FISCHER, qui figure inévitablement dans les présents balbutiements.

Double Chooz ne se limite pas au CEA; je tiens ainsi à mettre l'accent sur Romain RONCIN pour son entrain et son ouverture d'esprit, et sur Emmanuel CHAUVEAU pour sa disponibilité sur site et à distance, et ce à n'importe quelle heure! Merci également pour ce franc-parler si cocasse, ce goût pour les bonnes choses, et merci à l'humain qui se cache derrière le champ de compétences! En ce qui concerne les permanents de plus longue date, je ne saurais omettre l'IPHC et Cécile JOLLET-MEREGAGLIA, pour tous les échanges que nous avons eus sous son œil bienveillant. Je me dois également de remercier les membres de l'APC et Anatael CABRERA expressément pour sa confiance et son regard sur mon travail.

Not only did I have the chance to travel Europe extensively during this three-year undertaking, but I even got the opportunity to spend one month in one of the queerest countries

ACKNOWLEDGEMENTS

I have set foot in, i.e. Japan. For this invaluable and unforgettable experience, I would like to express my deepest gratitude to Masaki ISHITSUKA, without whose steady support, kindness, and open-mindedness, this exchange would have had a different taste. Many thanks also go to Michiru KANEDA for his help with the Japanese computing grid and for introducing Victoria and me to okonomiyaki! I owe Ralitsa SHARANKOVA much for fetching me at Haneda, and assisting me in the Tokyo underground and the O-Okayama Tokyu Store! Eventually, I am grateful to Masahiro KUZE for making my stay at Tokyo Tech possible.

I am deeply indebted to Susanne MERTENS for having shared her eye-opening experiences with me in Jyväskylä, and for having introduced me to Joseph FORMAGGIO in London, whom I thank sincerely for hiring me as a post-doctoral associate, thereby allowing me to tackle the question of neutrino masses.

Même si cet investissement ne figure pas, à proprement parler, dans ce document, je souhaite manifester toute ma gratitude à Sébastien DE ROSSI, qui m'a donné bien plus qu'un coup de pouce dans mes activités d'enseignement à travers les salles de SupOptique et du campus d'Orsay.

The motley crüe

En dépit de leur proximité géographique du lundi au vendredi (hors jours fériés et ponts CEA), j'ai rarement travaillé avec les personnes citées ci-dessous ; pourtant, elles ont eu leur influence, sinon sur le manuscrit, au moins sur l'auteur.

J'ai effectivement eu la chance de rompre le jeûne de midi régulièrement avec ces théoriciens aux personnalités si dépayssantes que sont Jaume CARBONELL et Pierre GUICHON ; plus souvent au CERN que Pierre n'est en Australie, j'ai tout de même largement bénéficié de la bonne humeur de Nicole D'HOSE. De la même manière, le rez-de-chaussée neutrino s'est vu renforcé fréquemment par Alain LETOURNEAU et Thomas MATERNA, dont les caractères si différents se conjuguent en une alchimie théâtrale, montrant ainsi un autre visage de la recherche.

Chaque découpage a ses limitations, et si Antoine COLLIN a su me mettre patiemment sur les rails de la recherche et partager – encore aujourd’hui – son expérience emplie de sagacité, je retiendrai également sa culture débordante, ses opinions originales et son entrain merveilleux par-delà les grillages du CEA. Une partie non négligeable des résultats de cette thèse a été obtenue alors que je partageais le bureau 30A avec Maxime PEQUIGNOT ; sa bonne humeur, son rire facile et sa tolérance ont grandement facilité le partage des parcelles fertiles du lot 30A ! Ce lopin de terre fécond n'a pas laissé indifférent Thibaut METIVET, dont les incursions répétées ont non seulement permis de redessiner le monde, mais m'ont également laissé apercevoir le vaste océan de possibilités offertes par le langage de Bjarne STROUSTRUP. Sans sa sensibilisation à l'esthétique de la pieuvre, sa disponibilité, ou sa pédagogie, je serais – sans l'ombre d'un doute – toujours en train « d'écrire du C++ comme du Fortran » ; il m'a appris à naviguer avec mes propres voiles, et même si je retrouve

ACKNOWLEDGEMENTS

régulièrement de l'eau sur le pont, le navire n'a pas encore chaviré ! Je finis par une pensée pour Adrien BLANCHET, arrivé dans le 30A en tant que stagiaire au moment le moins opportun : préparation de Neutrino 2016 et spectre du manuscrit omniprésent ; je ne crois pas m'égarer en affirmant que n'importe quelle cohabitation lui sera désormais charmante !

Presque occupant du 30A lui aussi, véritable onde plane du SPhN, c'est à Raphaël BRISELET qu'incombe la transition. Je ne boude pas mon plaisir face à son ouverture d'esprit, sa curiosité fantastique, son sourire indéfectible et le piment qu'apportent au SPhN ses goûts singuliers. Occupant le bureau de Raphaël avec une parcimonie garante de résultats élaborés, je n'oublie pourtant pas Maud AIRIAU et sa conversation facile. Nous talonnant d'une année, je remercie Loïc THULLIEZ pour sa motivation lors de nos excursions forestières et sa démarche initiatique ayant abouti à l'éclosion des « précaires du SPhN ». Amongst the great runners of our department, I would like to thank Michał RĄPAŁA for his easy-going yet discreet personality (sought-after skills on the office-sharing market). I truly enjoyed hearing his experience and discussing French, Polish and Brazilian ways. Dziękuję bardzo ! Indubitablement plus expansif que son homologue de l'est, la tournée des athlètes se poursuit avec Antoine VIDON, que je remercie vivement pour le torrent d'histoires poilantes qu'il apporte au moulin des discussions ! Grand chef, sportive de haut niveau, jardinier extraordinaire à ses heures perdues, je suis profondément reconnaissant envers Aurélie BONHOMME pour sa bienveillance bonhomme, son questionnement de l'ordre établi, ses talents de dessinatrice et le meilleur houmous de la région ! Pour avoir délicieusement partagé son vécu et son expérience de travail aux quatre coins du monde, pour le NFT de Boston et sa relecture stimulante des trois premiers chapitres de ce document, je remercie généreusement Nancy PAUL. Bande hétéroclite s'il en est, pour le moins charmante, je ne manque pas de mentionner les « théoriciens du fond », Pierre ARTHUIS, Benjamin BAILLY et Mehdi DRISSI. J'exprime toute ma sympathie envers le Barberousse du SPhN, Alessandro MINOTTI, pour ses avis tranchés comme par un sabre d'abordage, ses encouragements néanmoins affables et sincères, et ses propositions de sorties en pleine mer parisienne.

Le soutien indéfectible

Cette odyssée a été ponctuée d'escales en terres accueillantes, qu'elles soient musicalement fertiles, internationales, largement culturelles, ou qu'elles arborent les fruits bigarrés d'une longue amitié ; ces ports d'attache riment surtout avec : Sylvain, Théo, Alexis, Antoine, Geoffrey, Nathan. En particulier, je désire souligner la capacité d'écoute d'Antoine, sa ténacité et ses accueils répétés à Londres. Je voudrais également exprimer tout mon soutien à Alexis pour sa thèse, tout laisse à croire qu'il me rejoindra sans difficultés sous le dôme emblématique du MIT ; Boston s'ajoutera de bonne grâce à la liste des villes que nous avons conjointement foulées ! Naturligtvis har jag inte glömt ni, Birgit och Ben, det var jätteroligt att häンga ihop i Sverige och att träffas igen i Tyskland, vi hörs !

Le soutien de l'abbaye Notre-Dame-de-Saint-Rémy n'est pas en reste, et c'est principalement pour ce numéro 10 si onctueux et si parfumé – qu'il m'a été donné de déguster

ACKNOWLEDGEMENTS

régulièrement, grâce à la proximité providentielle de la congrégation avec le site de Chooz – qu'elle figure ici.

As a worthy substitute for coffee, I am acutely indebted to Ziggy Stardust, Tony Iommi, Phil Lynott, Steve Harris, Geddy Lee, Mikael Åkerfeldt, Robert Fripp, Steven Wilson, Gavin Harrison, Maynard James Keenan, Mike Vennart, Mariusz Duda, Sean Reinert, Don Anderson, Eric Jernigan, Chris Hrasky, Mike Patton, Sully Erna, Kevin K.R. Starrs, Black Francis, Robert Smith, Jack White, Dave Brubeck, Bill Evans.

Pour ses conseils et l'œil distant mais sûr qu'il a gardé sur moi, pour s'être montré disponible au cours de tous ces déménagements, je suis reconnaissant envers mon père. Je remercie ma petite soeur d'être venue me faire une surprise le 16 novembre, et ma mère, pour ses appels téléphoniques répétés !

Хоть и последняя, но не менее важная: моя любимая Вика, я никогда не смогу отблагодарить тебя за всё то, что ты для меня сделала, пока я писал диссертацию. Без сомнения, диссертация была бы совсем другой, если бы ты не отдавала мне своё свободное время и не была бы такой терпеливой. Теперь ты даже почти шеф-повар! Ты во всём мне помогала, не щадила себя и заплатила дорогую цену. Но благодаря аспирантуре, мы посетили так много стран и многое пережили! Большое тебе мерси, дорогая!

Contents

Introduction	1
I Neutrino physics	3
1 Admitting neutrinos in the field	5
1.1 Discovery	5
1.1.1 Conundrum and postulate	5
1.1.2 Compelling evidence	6
1.1.3 Detecting a poltergeist	6
1.2 First properties	8
1.2.1 Several neutrino flavours	8
1.2.2 Parity and handedness	9
2 Oscillating neutrinos	11
2.1 Experimental signs	11
2.1.1 Disturbing experimental data	11
2.1.2 Supporters	12
2.1.3 Crowning achievements	12
2.1.3.1 Solar neutrinos	12
2.1.3.2 Atmospheric neutrinos	13
2.1.3.3 Anthropogenic neutrinos	16
2.2 Theory of neutrino oscillations	17
2.2.1 First draft	17
2.2.2 Mixing matrix	18
2.2.2.1 Two-dimensional formalism	18
2.2.2.2 Three-dimensional case	19
2.2.3 Quantum-mechanical approach	21
2.2.3.1 Plane wave derivation	21
2.2.3.2 Ultra-relativistic approximation	22
2.2.3.3 Oscillation probabilities with trigonometric functions	23
2.2.3.4 Survival probability	24

2.3	Parameters of the model	24
2.3.1	Neutrino masses	24
2.3.1.1	Individual masses	24
2.3.1.2	Squared mass differences	25
2.3.2	Matrix coefficients	26
2.3.2.1	Large mixing angles	26
2.3.2.2	Minute mixing angle	27
2.3.2.3	CP violation phase	30
II	Neutrinos in Double Chooz	33
3	$\bar{\nu}_e$ production at Chooz	35
3.1	Production site	35
3.2	Nuclear fission	36
3.2.1	Overcoming the Coulomb barrier	36
3.2.2	Chain reaction in nuclear reactors	37
3.2.3	Reactor fuel composition	38
3.3	$\bar{\nu}_e$ release	40
4	$\bar{\nu}_e$ detection	43
4.1	Reaction	43
4.1.1	Signature	43
4.1.2	Threshold	45
4.1.3	Energy relations	46
4.1.3.1	$\bar{\nu}_e$ energy	46
4.1.3.2	Visible energy	47
4.1.3.3	Visible energy at zeroth-order	47
4.1.4	Cross-section	48
4.2	Detector positioning	50
4.2.1	Striking a balance	50
4.2.2	Averaged oscillation	51
4.2.3	Overburden values	51
4.3	Detector design	51
4.3.1	Inner Detector	52
4.3.1.1	Neutrino Target (1)	52
4.3.1.2	Gamma Catcher (2)	54
4.3.1.3	Buffer (3)	55
4.3.2	Additional shieldings	56
4.3.2.1	Inner Veto (5)	56
4.3.2.2	Passive shielding (6)	57

CONTENTS

4.3.2.3	Outer Veto (7)	58
4.3.3	Calibration systems	58
4.3.3.1	Light injection system	58
4.3.3.2	Target calibration system (z -axis)	59
4.3.3.3	Gamma Catcher calibration system (Guide Tube)	59
4.3.3.4	Artificial sources	62
4.4	Data acquisition	63
4.4.1	ν -DAQ	63
4.4.2	OV-DAQ	64
5	Flux prediction and event reconstruction	65
5.1	Prediction	65
5.1.1	$\overline{\nu_e}$ flux	65
5.1.1.1	Fission rate	65
5.1.1.2	Fractional fission rates	66
5.1.1.3	Infinitesimal flux	67
5.1.1.4	Reference spectra	67
5.1.2	Expected signal	69
5.1.2.1	Differential form	69
5.1.2.2	Binned expected antineutrino rate	70
5.1.2.3	Total binned antineutrino count	70
5.1.3	Monte-Carlo Signal	71
5.1.3.1	Random generation of events	71
5.1.3.2	Main simulation	72
5.1.3.3	Quenching model	72
5.1.3.4	Readout and common algorithms	75
5.2	Event reconstruction	76
5.2.1	Charge and time	76
5.2.2	Position	77
5.2.2.1	Principle	77
5.2.2.2	Maximum likelihood estimation	77
5.2.2.3	Resolution	78
5.2.3	Energy	78
5.2.3.1	Finding the number of photo-electrons	79
5.2.3.2	Spatial uniformity	82
5.2.3.3	Absolute energy scale	83
5.2.3.4	Corrections	84
5.2.4	Muon tracks	90
5.2.4.1	Making choices	90
5.2.4.2	Estimation method	90
5.2.4.3	Performance	91

CONTENTS

6 Measuring θ_{13}	97
6.1 Event selection	97
6.1.1 Singles	97
6.1.1.1 Muon	97
6.1.1.2 After muons	98
6.1.1.3 Light noise	99
6.1.1.4 Energy range and summary	101
6.1.2 Pairs	101
6.1.2.1 Space-time correlation	101
6.1.2.2 Energy windows	102
6.1.2.3 Isolation cut	103
6.2 Backgrounds	103
6.2.1 Accidental background	103
6.2.2 Fast neutrons and stopping muon's	104
6.2.2.1 Stopping muons	105
6.2.2.2 Fast neutrons	108
6.2.3 Cosmogenic background	109
6.3 Oscillation fit	111
6.3.1 Formulation	111
6.3.1.1 Strategy	111
6.3.1.2 Least squares	111
6.3.2 Uncertainties and correlations	113
6.3.2.1 Backgrounds	113
6.3.2.2 Reactor	115
6.3.2.3 Detection	115
6.3.2.4 Energy	117
6.3.3 Fit results and prospects	118
6.3.3.1 Best fit	118
6.3.3.2 Comparison to the $\bar{\nu}_e$ survival probability	119
6.3.3.3 Double Chooz amongst others	121
III Cosmogenic background studies	123
7 Generating cosmogenic decays	125
7.1 Generating each raw decay	125
7.1.1 Handling strong decays	126
7.1.1.1 Two-body decays	126
7.1.1.2 Many-body decays	127
7.1.2 Processing β - decays	131
7.1.2.1 Obtaining the kinetic energy of an electron	131

CONTENTS

7.1.2.2	Alleged classification of the β -decays	132
7.1.2.3	Accounting for the width of the daughter nucleus	133
7.2	Simulating a raw event	135
7.2.1	First decays	135
7.2.1.1	Decay schemes	135
7.2.1.2	Rest decays	137
7.2.2	Dealing with resonant states	138
7.2.2.1	Non relativistic Breit-Wigner distribution	138
7.2.2.2	Issues with the non-relativistic Breit-Wigner distribution .	139
7.2.2.3	Gaussian modelling	140
7.2.3	The chain constraints	142
7.2.3.1	Sequential processing	142
7.2.3.2	Synchronous processing	143
7.2.4	Position of the event	144
7.2.4.1	Carbon share	144
7.2.4.2	Position generation	145
8	Obtaining predicted spectra	147
8.1	Handling the decay trees	148
8.1.1	Generating a raw spectrum	148
8.1.1.1	Input	148
8.1.1.2	Processing	148
8.1.1.3	Saving the output	149
8.1.2	Generating individual branches	149
8.1.2.1	Specifying the parameters in the raw generator	149
8.1.2.2	Simulating the detected branches	149
8.1.3	Applying the analysis cuts	150
8.1.3.1	Definition	150
8.1.3.2	Impact	151
8.1.3.3	Spectra database	153
8.2	Reconstructing a mean spectrum with errors	155
8.2.1	Vary that which thou canst not set	156
8.2.1.1	Ratio modelling	156
8.2.1.2	Weighting the detected spectra database	156
8.2.2	Updating a covariance matrix	157
8.2.2.1	Recurrence relation for the covariance matrix estimator . .	157
8.2.2.2	Convergence test	158
8.2.3	Weak magnetism uncertainty	161
8.3	Combining spectra from disjoint sets	163
8.3.1	Ratio uncertainties	163
8.3.2	Weak magnetism uncertainty	164

CONTENTS

8.3.3	Linear combination of spectra	164
8.4	Results and spectra comparison for ${}^8\text{He}$ and ${}^9\text{Li}$	165
8.4.1	Mean spectra	165
8.4.1.1	Gd analysis	165
8.4.1.2	H analysis	167
8.4.2	Covariance and correlation matrices	169
8.4.2.1	Gd analysis	169
8.4.2.2	H analysis	173
8.4.3	Conclusion	175
9	Extracting spectra from data	177
9.1	Cosmogenic veto	177
9.1.1	Targeted events	177
9.1.2	Formulation	178
9.1.2.1	Likelihood	178
9.1.2.2	Posterior probability	178
9.1.2.3	Usage	179
9.1.3	Priors	180
9.1.3.1	Cosmogenic prior	180
9.1.3.2	Prior ratios	181
9.1.4	Reference probability densities	182
9.1.4.1	Independent variables	182
9.1.4.2	Distance to μ -tracks	182
9.1.4.3	Neutron multiplicity	183
9.2	Vetoed signal	187
9.2.1	Background subtraction	187
9.2.1.1	Principle	187
9.2.1.2	Practical constraints	188
9.2.1.3	Improved accidental background removal	189
9.2.1.4	Correlated background	191
9.2.2	Veto performance	192
9.2.2.1	Retrieving characteristic quantities	192
9.2.2.2	Preparing for the near site	193
9.2.2.3	Cosmogenics and accidentals at ND	195
9.2.3	Selected threshold	198
9.2.3.1	Providing the best constraining spectrum	199
9.2.3.2	Vetoed rates	200
9.2.3.3	IBD inefficiencies	201
9.3	Spectral analysis	202
9.3.1	Compatibility across detectors	202
9.3.1.1	Graphical appetiser	202

CONTENTS

9.3.1.2	χ^2 test for homogeneity	203
9.3.1.3	Kolmogorov-Smirnov test	204
9.3.2	Comparison to Monte-Carlo predictions	205
9.3.2.1	χ^2 fit	206
9.3.2.2	Fit results	207
9.3.2.3	${}^8\text{He}$ fraction	209
10	Rate estimations	213
10.1	Some estimation methods	213
10.1.1	Principle	213
10.1.2	Maximum posterior probability approach	214
10.1.3	Lateral distance approach	215
10.1.3.1	Envelope functions	215
10.1.3.2	Characteristic production length estimation	216
10.1.3.3	Total cosmogenic rate and prospects	217
10.2	Muon sample cleansing	218
10.2.1	Analysis method	218
10.2.1.1	Neutron multiplicity threshold	218
10.2.1.2	Fitting the time intervals	219
10.2.1.3	After- μ veto	219
10.2.2	Results	220
10.2.2.1	Far detector	220
10.2.2.2	Near detector	221
10.2.2.3	Rates summary	222
10.3	Candidate sample cleansing	222
10.3.1	Method	223
10.3.1.1	Motivations and past achievements	223
10.3.1.2	Monte-Carlo correction	223
10.3.2	Application	225
10.3.2.1	Total far detector rates	225
10.3.2.2	Efficiency of the multiplicity cut	228
10.3.2.3	Near detector	230
10.4	Final rates	233
10.4.1	Remaining rates	233
10.4.2	Comparison	234
IV	Relative normalisation of the $\overline{\nu_e}$ rates	237
11	Weight measurements	239
11.1	Performing a weight measurement	239

CONTENTS

11.1.1 Principle	239
11.1.2 Standards	240
11.2 Near detector data analysis	240
11.2.1 Weight measurement	240
11.2.1.1 Full weighing tank	240
11.2.1.2 Target filled	242
11.2.2 Target mass estimation	244
11.2.2.1 Sensors	245
11.2.2.2 Nitrogen	245
11.2.2.3 Filling tube	246
11.2.2.4 Target mass value after filling	247
11.2.3 Target mass evolution and number of protons	247
11.2.3.1 Vessel expansion	247
11.2.3.2 Liquid expansion	247
11.2.3.3 Overall evolution	248
11.2.3.4 Number of target protons	248
11.3 Far detector data re-analysis	249
11.3.1 Weight measurement	249
11.3.1.1 Weighing tank loading	250
11.3.1.2 Full weighing tank	250
11.3.1.3 Target filled	252
11.3.2 Target mass estimation	254
11.3.2.1 Sensor drift	254
11.3.2.2 Gravity correction	256
11.3.2.3 Nitrogen	256
11.3.2.4 Filling tube	257
11.3.2.5 Target mass value after filling	257
11.3.3 Target mass evolution and number of protons	257
11.3.3.1 Overall evolution	257
11.3.3.2 Number of protons	257
11.4 Main achievements	258
Conclusion	261

Introduction

In the bestiary of elementary particles, neutrinos are quaint creatures. These neutral leptons are so elusive that they might be qualified as bystanders of particle physics, yet nothing could be further from the truth. In fact, their etherealness is rivalled but by their abundance and nearly lightning-fast speed, i.e. properties which make them ideal candidates for studying locations humanly inaccessible, be they stars, the core of the Earth, or man-made sources of energy such as nuclear power plants.

By all manner of means, neutrinos themselves come with their own secrets, and the more we learn about these messengers of new physics, the less we doubt their peculiarity. Although theories can accommodate for them by minimal extensions, it seems as though something is awry. For indeed, their individual masses, albeit unmeasured, are unquestionably small, suspiciously small. By the same token, neutrinos mingle amongst one another, in a fickle manner, presenting the largest mixing between particle species ever observed. If that was not enough, antineutrinos and neutrinos seemingly mix in different ways, which heralds consequences all the greater that these neutral fermions exist in copious quantities throughout the universe.

For all these prospects, we must first ensure that the gateway to further knowledge, i.e. the value of the smallest mixing parameter θ_{13} , is not biased. Quite apposite in the year 2016, let us emphasise that, like when attributing Nobel prizes, great care must be taken that values – or discoveries – have been cross-checked and identically observed by other experiments. Double Chooz gave the first direct indication of the non-zeroness of θ_{13} with reactor antineutrinos, and like other experiments, it still strives to refine the significance of its measurement.

Accurately measuring θ_{13} is no leisurely stroll, and the difficulty of such an endeavour is underscored by the length of this document. The latter is divided into four parts, of varying lengths.

The first part reviews the main properties of neutrinos by way of two chapters. Chapter 1 focuses on the discovery and first properties of neutrinos, while Chapter 2 introduces the neutrino oscillation phenomenon and eventually derives the antineutrino oscillation probability relevant to this thesis.

Part II is set on presenting a detailed picture of the Double Chooz experiment, from the production of electron antineutrinos (Chapter 3), to the design of the two detectors with which they may interact (Chapter 4). Additionally, in Chapter 5, the antineutrino production

INTRODUCTION

model to which the recorded events are compared, along with the reconstruction algorithms, are reviewed. After the analysis cuts have separated the wheat from the chaff, the actual measurement of $\sin^2(2\theta_{13})$ – by means of a multi-detector configuration – is performed in Chapter 6.

Part III is dedicated to the background dominating the uncertainty on the $\sin^2(2\theta_{13})$ measurement from Chapter 6, caused by the decays of cosmogenic isotopes within the detector itself. These decays, that hamper the reliability of the antineutrino spectra, are simulated in Chapter 7. The building of spectra from these simulated events, complemented by a thorough error treatment, is presented in Chapter 8. The corresponding decays are partially selected within the data samples by dint of a cosmogenic veto, the performance of which is discussed in-depth in Chapter 9, for both detectors. The assessment of the rate of cosmogenic background remaining after the veto has been applied is the main topic of Chapter 10.

Chapter 11 is a loner in its Part IV, albeit no less stirring, for it addresses the absolute and relative normalisations of the antineutrino rates observed in both detectors.

Part I

Neutrino physics

Chapter 1

Admitting neutrinos in the field

Nowadays, neutrinos are perfectly valid contenders of the particle physics playground, and one may dare say, amongst the top-rated and most exciting players of the beginning of the twenty-first century. Now is also the time to remember that it has not always been like that. Not only did we not know that they came in several species – the number of which still being subject to debate – but a mere century ago, neutrinos we regarded as a pure construct of the mind, even for eminent physicists such Niels Bohr. At best, neutrinos were bookkeeping devices to rescue the conservation laws. And yet, if they would safeguard the energy conservation law, they would also emphasise parity violation, and even be detected with a different flavour than that with which they had been produced. But before studying neutrino oscillations, which we save as the main topic for Chapter 2, let us go back in time to the theoretical birth of this exceedingly abundant particle the neutrino is.

1.1 Discovery

1.1.1 Conundrum and postulate

Less than twenty years after the discovery of natural radioactivity by Henri Becquerel [1], the continuous nature of β -spectra was exhibited by James Chadwick in 1914 [2]. The kinematics of two and many-body decays will be extensively reviewed in part III, but it is not too much of a forecast to point out that two-body decays are characterised by a spectrum showing two distinct kinetic energy peaks. The disagreement between the experimental evidence and the two-body decay assumption

$$X \rightarrow Y + e^-, \quad (1.1)$$

where X stands for the decaying nucleus, Y its daughter, e^- the ejected electron, could not have been greater.

Undoubtedly, a third particle had to be involved in β -decays. This particle had to be neutral to conserve charge and remain hardly detectable. It must also be extremely

lightweight, for occasionally, there is no missing energy so that the maximum kinetic energy T_e^{max} available for the electron is

$$T_e^{max} = m_X - m_Y - m_e, \quad (1.2)$$

which still holds up to the accuracy of current measurements, with m indicating the nuclear masses. Besides, it must carry a 1/2 spin to ensure the latter is conserved (thus, coupling with the electron would result in a 0 or 1 spin). Such a candidate was originally labelled "neutron" by Wolfgang Pauli, in 1930, in the originally-derided "Liebe Radioaktive Damen und Herren" open letter [3]. However, the "neutron" as we picture it today, would be discovered in 1932 by James Chadwick [4], and appear as far too heavy a fermion to meet Pauli's requirements. Enrico Fermi made the most of it all and offered, at the turn of the following year [5]¹, a theory of β -decay so successful that Pauli's suggestion eventually had to be taken seriously. Thereafter, the lightweight neutral fermion, enforcing energy and spin conservation in β -decays, was labelled "neutrino" (symbol ν), from the Italian equivalent of "small neutron". Thus, the theoretical postulate – that " ν " embodies – corrects (1.1) into

$$X \rightarrow Y + e^- + \nu. \quad (1.3)$$

1.1.2 Compelling evidence

Thanks to Fermi's theory, which can truly be regarded as a cornerstone in the building of the Standard Model, the theoretical foundations for the role of neutrinos had been laid. In 1947, the missing particles on the photographic emulsions of Cecil Frank Powell, that lead to the discovery of pions (π) [6], was more compelling evidence for the existence of neutrinos, as highlighted in the decay of the former into muons (μ)

$$\pi \rightarrow \mu + \nu. \quad (1.4)$$

Less than three years later, the spectrum of the subsequent muon decay was confirmed to be continuous, with a mean energy of 34 MeV and an endpoint of 55 MeV [7]², thereby leaving room for two neutrinos

$$\mu \rightarrow e + \nu + \nu. \quad (1.5)$$

1.1.3 Detecting a poltergeist

Despite the theoretical motivations, there remained to directly detect this ghost particle, for it left no tracks, and did not decay. If truth be told, no one had every seen a neutrino do

¹The first iterations appear in Italian and German journals because the famous Nature journal had deemed Fermi's theory "too remote from reality".

²Which is in stunningly good agreement with what is reconstructed from such decays in the Double Chooz detectors.

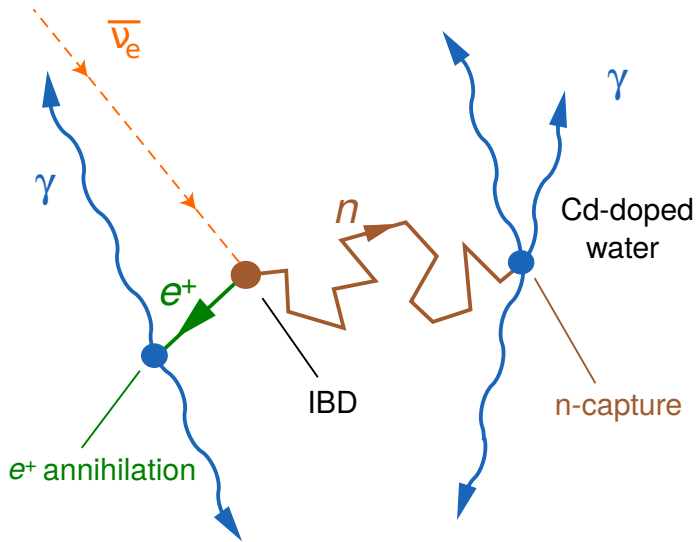


Figure 1.1 – Reactor antineutrino detection method used by F. Reines and C. L. Cowan at the Hanford and Savannah River experiments. Antineutrinos interact with water protons through inverse β -decay. The emitted e^+ annihilates with an e^- of the medium, and a few microseconds after, the n is captured by a Cd nucleus, which in turn, emits several γ 's. The γ 's can be detected thanks to horizontal liquid scintillator tanks not drawn on the schematic.

anything. And yet, as Fermi's interaction predicts, it should interact with a target full of water (and therefore of protons p) through the so-called "inverse β -decay"

$$p + \bar{\nu} \rightarrow n + e^+, \quad (1.6)$$

thereupon emitting a neutron (symbol n) and Dirac's positron (symbol e^+). In equation (1.6), we took a step forward by enforcing the antimatter character of the neutrino involved in this decay. This distinction first appears experimentally in 1955, when Raymond Davis reported his failed attempt to detect antineutrinos ($\bar{\nu}$) – allegedly emitted by the Brookhaven nuclear reactor – using the neutrino-sensitive reaction [8]



that was first advocated by Bruno Pontecorvo [9]³. In order to unambiguously detect the interaction of the antineutrino with a proton from a water tank, both the double coincidence between a prompt and a delayed event (see Figure 1.1) and a significant shielding to cosmic rays, were crucial.

Indeed, if the requirement of a time coincidence between the annihilation of the positron and the capture of the neutron – a technique still put to good use in Double Chooz (with Gd

³Before he left Canada for USSR in 1950, B. Pontecorvo had initiated the building of a neutrino detector using the Chlorine-Argon technique at the Chalk River laboratory.

instead of Cd, cf. Chapter 4) – removes a large amount of background, in 1953, at the ^{239}Pu -producing Hanford reactor, the overwhelming rate of cosmic muons prevented Clyde Lorrain Cowan and Frederick Reines from detecting the antineutrino with enough significance [10]. On the other hand, when C. L. Cowan and F. Reines moved to the better shielded Savannah River experimental site, with a detector design aimed at rejecting backgrounds, they could detect a reactor-power dependent signal in good agreement with the predicted cross-section [11]. The antineutrino had been discovered.

1.2 First properties

1.2.1 Several neutrino flavours

Along with the experimental progress to detect (anti)neutrinos, theoretical works, initiated by E. J. Konopinski and H. M. Mahmoud [12], had introduced a quantity L , which we now call "lepton number". This supposedly conserved number evaluates to $L = 1$ for neutrinos and negatively charged leptons, and $L = -1$ for antineutrinos and the positively charged leptons. From that, it is clear that the Chlorine-Argon technique from (1.7) is insensitive to antineutrinos. Nevertheless, the theoretically allowed process

$$\mu \rightarrow e + \gamma \quad (1.8)$$

had never been observed [13], and the experiment was in accordance with process (1.5), hence suggesting the existence of different lepton numbers for different "kinds", or rather "flavours", of particles : L_e and L_μ at that time. Such an assumption implied that there were not only neutrinos and antineutrinos out there, but in fact, several flavours of them, as discussed in detail by B. Pontecorvo [14]. This hypothesis was confirmed by the 1962 Brookhaven experiment [15], in which muon (anti)neutrinos – produced by pion and kaon decays – successfully produced muons through

$$n + \nu_\mu \rightarrow p + \mu^- \quad (1.9)$$

$$p + \overline{\nu_\mu} \rightarrow n + \mu, \quad (1.10)$$

but during which the forbidden processes

$$n + \nu_\mu \rightarrow p + e^- \quad (1.11)$$

$$p + \overline{\nu_\mu} \rightarrow n + e^+, \quad (1.12)$$

were not observed in meaningful amounts. Everything comes in threes, at least that much can be said of the neutrinos that interact with the weak interaction⁴, and a few decades later, the ν_τ was found by the DONUT collaboration [16].

⁴This thesis shall eagerly refrain itself from opening the "sterile neutrino" can of worms before the hurly-burly's done.

1.2.2 Parity and handedness

As emphasised in 1956 by T. D. Lee and C. N. Yang, the so-called " $\tau - \theta$ puzzle" was but an incentive to study parity violation in the weak interaction [17]; no experiment determining whether this interaction differentiated the right from the left, had ever been performed. Mathematically speaking, the parity operator changes the sign of all the spatial coordinates, and hereby the direction of motion of particles. The parity operator leaves the spin direction unchanged, thus, aligning the spin of particles or nuclei in the direction opposite to their previous ones, while retaining the observation along the same spatial direction, is effectively a parity transformation. Observing an asymmetric behaviour in the β -decays of nuclei, when reversing the direction of the magnetic field polarising them, is consequently a proof of parity violation.

Examining the parity conservation in β -decays requires an allowed⁵ transition, with a spin change $\Delta J = 1$, so that the electron and the antineutrino always align the spin they carry away with that of the daughter nucleus. Moreover, orienting the spins of nuclei demands a H/T ratio (with H the magnetic field, and T the temperature) so high to overcome the tiny value of the Bohr magneton μ_B , that nuclei with a large coupling between the nuclear spin and the electronic moment had to be used. On top of having a relatively manipulable half-life of 5.27 y, the $J^\pi = 5^+$ (with π the parity of the state) ground state of ${}^{60}\text{Co}$, which mainly β -decays to the 4^+ state of ${}^{60}\text{Ni}$ in



meets all the aforementioned requirements. An asymmetry between the number of detected electrons when polarizing the ${}^{60}\text{Co}$ upwards or downwards was observed by Chien-Shiung Wu in 1957 [18]. It follows that the antineutrino is always⁶ emitted in the half-space into which the ${}^{60}\text{Ni}$ spin points, the direction of which being identical to its polarized ${}^{60}\text{Co}$ mother. Recalling that the spin of the antineutrino is aligned with the ${}^{60}\text{Ni}$ spin, it means that its helicity – defined as the sign of the projection of the spin on the direction of motion – is always positive (see Figure 1.2).

A few months later, M. Goldhaber confirmed that the neutrino emitted in the electron capture reaction



had a negative helicity [19]. In a nutshell, neutrinos are left-handed, and antineutrinos are right-handed. It was natural to assume that neutrinos were massless, for in addition of the apparent mass conservation in β -decays (see 1.1.1), massive neutrinos could have been overtaken by a Lorentz boost.

⁵In allowed decays, the electron and the antineutrino do not carry any orbital angular momentum, which unambiguously determines the direction of their spins.

⁶Due to the difficulty of aligning all the spins of all the nuclei, C. S. Wu could only observe a significant asymmetry.

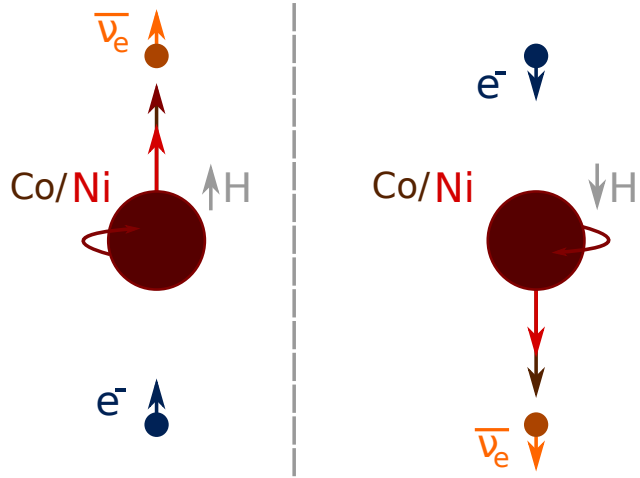


Figure 1.2 – In the β -decay of ^{60}Co into ^{60}Ni , the electrons are emitted in the direction opposite the nuclear spins – which have been polarized by a magnetic field H – and the antineutrinos, thus, have a positive helicity. Spin conservation is emphasised by the colourful arrows.

Undoubtedly, the weak interaction – that is to say, the only interaction through which neutrinos interact – does not conserve parity. It is worthwhile noting that although the mirror image of the left-handed neutrino is the yet to be detected right-handed neutrino, combining the charge conjugation C – which turns matter into anti-matter – with the parity operator P , does output a particle we are well acquainted with : the right-handed antineutrino. Obviously, it took us but a few more years to understand that the CP symmetry was not a symmetry good enough for this world, at least that much can be said for mesons [20]; the measurement to which this thesis contributes, is closely related to the global picture.

Chapter 2

Oscillating neutrinos

If it were not for neutrinos, the Standard Model, as formalised in the sixties for its electroweak part, and in the seventies for its strong interaction component, would hold in triumph, and the 2012 discovery of the Higgs particle would but vouch for it. However, over the last two decades, irrefutable evidence for neutrino oscillations has been exhibited by several collaborations of physicists spread across the terrestrial globe, using either natural or man-made neutrino sources. Neutrino oscillations were world-acknowledged by the 2015 Nobel prize in Physics, attributed to Takaaki Kajita and Arthur B. McDonald, pillars of the Super-Kamiokande and SNO experiments, respectively. The oscillation phenomenon is not highlighted so much for it is the main topic of this thesis, but rather because it unequivocally proves that neutrinos have a mass, and in doing so, unveils a new area of physics beyond the Standard Model. Therefore, building up an increasingly accurate knowledge of the parameters characterising neutrino oscillations, amongst which θ_{13} is a peculiar contender, paves the way for a better understanding of the physical world.

2.1 Experimental signs

2.1.1 Disturbing experimental data

Parity violation favoured the development of chiral symmetries in which neutrinos were massless [21, 22]. And yet, disturbing data started to accumulate at the end of the sixties, shaping what would be referred to as the "solar neutrino problem".

Indeed, the very same Raymond Davis who had confirmed the impossibility to detect reactor antineutrinos with the Chlorine-Argon technique (see 1.1.3), turned his attention [23] to the number of neutrinos emitted by nuclear fusion inside the sun. To do so, R. Davis and his colleagues placed their 380 m^3 tetrachloroethylene Brookhaven detector at the Homestake Gold Mine, 1478 m below the surface, and for more than a decade, issued frequent reports [24, 25] acknowledging a two-third deficit in the rate of detected neutrinos, when compared to the predictions of John Bahcall [26, 27]. The detected rate was exceedingly low and

about one ^{37}Ar atom was produced every two days, which had to be collected regularly by helium purging, to examine its subsequent decay through electron capture. Of course, such an indirect radiochemical method, along with the expected low rate, arose doubts amongst experimentalists. Similarly, the solar model was called into question [28], and the rather high energy threshold of the Chlorine detection method limited the comparison to the production of ^8B in the sun¹, which is far from dominant.

2.1.2 Supporters

More than twenty years after it had recorded its first neutrino, the Homestake experiment eventually saw its results backed by data from the Kamiokande and Baksan detectors.

In 1990, through the use of elastic scattering on electrons

$$\nu + e^- \rightarrow \nu + e^-, \quad (2.1)$$

the Japanese water Cherenkov² detector measured the boron-related neutrino flux, and found it to be $0.46 \pm 0.05(\text{sys.}) \pm 0.06(\text{stat.})$ of the value predicted by the solar model [29]. At this point, it is apposite to stress that if elastic scattering on electrons can proceed via the weak interaction mediator Z^0 for all neutrino flavours, there is an extra Feynman diagram mediated by the W boson for ν_e . Therefore, if a part of the ν_e flux had converted – or oscillated – to other flavours, the total neutrino flux could not be assessed, unless one were to rely on the charged current results from Homestake to isolate the ν_e contribution [30], which was not a persuasive disentangling procedure to all.

On the other hand, the Soviet-American Gallium Experiment (SAGE), sensitive also to low-energy neutrinos released by deuteron production³ in the sun – which account for more than 90% of the solar neutrino production, and are less dependant on solar models than boron-induced neutrinos – reported a neutrino-capture rate from

$$^{71}\text{Ga} + \nu_e \rightarrow ^{71}\text{Ge} + e^-, \quad (2.2)$$

40% lower than its prediction with a 90% confidence level [31]. At Gran Sasso, the GALLEX experiment would soon swell the ranks of the Gallium supporters [32].

2.1.3 Crowning achievements

2.1.3.1 Solar neutrinos

If the aforementioned experiments had put the lid on the coffin of the solar neutrino problem, the Canadian Sudbury Neutrino Observatory (SNO) genuinely nailed the pine box. When

¹The signal comes from the β^+ -decay of ^8B into ^8Be , which is accompanied by the emission of a ν_e .

²Pet peeve: great diligence is often taken to substitute "Ch" for "Č", thereby heralding a stylistic Czech or Slovak transcription, but let us emphasise that the Nobel laureate is actually Russian.

³Two protons fusion into a deuteron, thereby emitting a ν_e .

2.1. EXPERIMENTAL SIGNS

conceding that neutrinos change flavour according to the oscillation mechanism, one must needs design an experiment able to detect all species with the same efficiency. In addition, the original sun-produced ν_e 's must be counted over the same period of time, to compare both fluxes unambiguously. To do so, SNO made the most of the relatively low break-up threshold of deuteron's (d):

$$d + \nu \rightarrow n + p + \nu, \quad (2.3)$$

a process equally sensitive to all flavours (only the Z^0 diagram is available to ν_e 's), and for which neutron emission is a characteristic signature. Moreover, since the incoming neutrinos do not have a kinetic energy large enough to produce heavy leptons, the charged current channel

$$d + \nu_e \rightarrow p + p + e^-, \quad (2.4)$$

is – as made explicit – relevant to ν_e 's only. The cherry on the cake is neutrino detection via elastic scattering on electrons (2.1), as in the Kamiokande (and their upgraded Super-Kamiokande version) detectors, which allows to cross-check the purely neutral and charged current channels. Taking into account the available Feynman diagrams, the expected fluxes from equations (2.3), (2.4) and (2.1), respectively read

$$\phi_{neutral} = \phi_{\nu_e} + \phi_{\nu_\mu} + \phi_{\nu_\tau} \quad (2.5)$$

$$\phi_{charged} = \phi_{\nu_e} \quad (2.6)$$

$$\phi_{elastic} = \phi_{\nu_e} + 0.15 (\phi_{\nu_\mu} + \phi_{\nu_\tau}) \quad (2.7)$$

A last, in 2002, by means of a 1kt spherical heavy water detector [33], located 2039 m below the surface, SNO published the following flux measurements

$$\phi_{neutral} = 5.09^{+0.44}_{-0.43} (\text{stat.})^{+0.46}_{-0.43} (\text{syst.}) \quad (2.8)$$

$$\phi_{charged} = 1.76^{+0.06}_{-0.05} (\text{stat.})^{+0.09}_{-0.09} (\text{syst.}) \quad (2.9)$$

$$\phi_{elastic} = 2.39^{+0.24}_{-0.23} (\text{stat.})^{+0.12}_{-0.12} (\text{syst.}) . \quad (2.10)$$

Without reserve, all the previous experiments had seen a deficit because all but a third of the ν_e 's produced by fusion reactions in the sun, had oscillated to the muon or tau flavour. As if that was not enough, the total neutrino flux was in conformity with the solar standard model [34].

2.1.3.2 Atmospheric neutrinos

Assuredly, the sun is not the only supplier of neutrinos and these neutral fermions are also produced in copious quantities in the upper atmosphere, particularly owing to high energy protons hitting air molecules, whereby pions are created (see Figure 2.1). Setting the right flavours on the pion and subsequent muon decays, we find

$$\begin{aligned} \pi^+ &\rightarrow \mu^+ + \nu_\mu & \Rightarrow & \mu^+ \rightarrow e^+ + \nu_e + \bar{\nu}_\mu \\ \pi^- &\rightarrow \mu^- + \bar{\nu}_\mu & & \mu^- \rightarrow e^- + \bar{\nu}_e + \nu_\mu . \end{aligned} \quad (2.11)$$

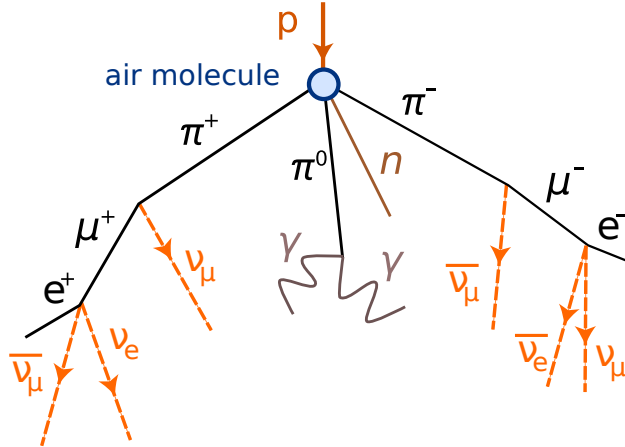


Figure 2.1 – Production of electron and muon neutrinos and antineutrinos in the upper atmosphere by bombardment of high energy protons.

Discarding neutrino oscillations for a just an moment, one would expect the ratio of the number of muon neutrinos (and antineutrinos alike) over that of electron neutrinos, to be close to 2, as is clear according to (2.11). The role of atmospheric kaons and the highly suppressed pion decays with an electron flavour are hereby overlooked, but this does not change the argument. In 1998, by way of charged currents – allowing flavour identification via the emitted charged lepton – the 50 kt water Cherenkov detector of Super-Kamiokande reported with great accuracy the value of the R ratio [35]

$$R = 0.63 \pm 0.03(\text{sys.}) \pm 0.05(\text{stat.}) . \quad (2.12)$$

The R quantity is defined as the data to Monte-Carlo ratio

$$R = \frac{N_\mu N_e^{MC}}{N_e N_\mu^{MC}} \simeq \frac{N_\mu}{N_\mu^{MC}}, \quad (2.13)$$

with N standing for the sum of the number of neutrinos and antineutrinos. To put it differently, nearly half of the muon (anti)neutrinos were missing with respect to the prediction, and their oscillation to the tau flavour was a competing explanation.

Furthermore, the Super-Kamiokande collaboration was able to detect the direction of the incoming neutrinos. Neutrinos coming downwards onto the detector travel a distance that is of the order of $L = 10$ km, on the other hand, neutrinos coming upwards have travelled a distance of the order of $L = 10\,000$ km. Thus, defining a quantity that is a function of the zenith angle θ (cf. Figure 2.2), directly challenges the alleged distance-dependence of neutrino oscillations. The asymmetry A embodies such a quantity, it is defined as

$$A = \frac{N_U - N_D}{N_U + N_D}, \quad (2.14)$$

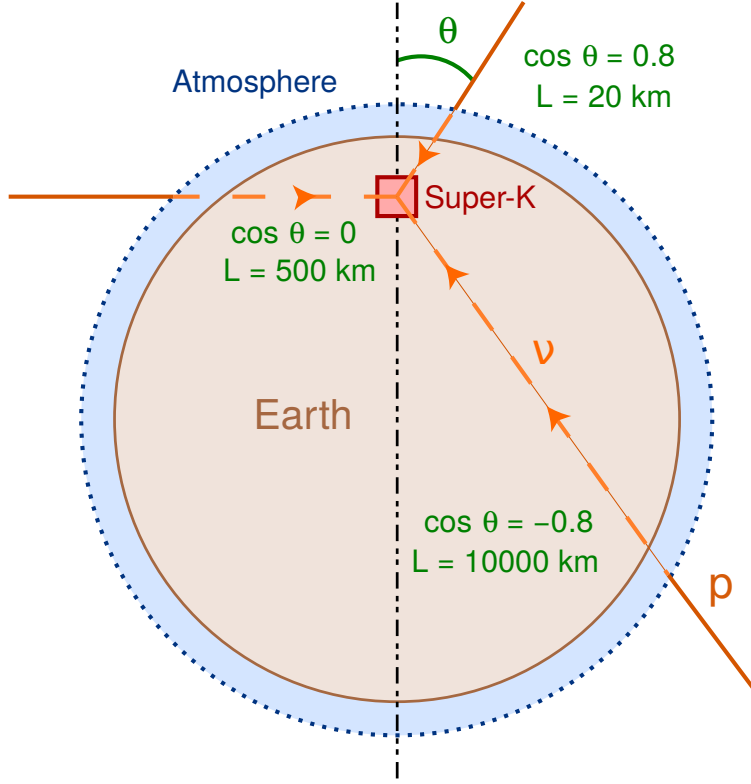


Figure 2.2 – Distance travelled by incoming atmospheric neutrinos as function of the cosine of the zenith angle θ , whose value is defined with respect to the axis of the Super-Kamiokande cylindrical detector. Thus, downward neutrinos have a positive cosine, and neutrinos coming upwards have a negative one.

where N_U and N_D are the number of upward and downward⁴ events, respectively. If the asymmetry for electron-like events is consistent with zero (see [35]), and therefore no oscillations of electron neutrinos presumably happen, muon-like events with an energy larger than 1330 MeV exhibit a staggering asymmetry

$$A = -0.296 \pm 0.048(\text{sys.}) \pm 0.01(\text{stat.}) , \quad (2.15)$$

which deviates from zero by more than 6 standard deviations. Although Super-Kamiokande did not quite solve the solar neutrino problem, it did bear the most conclusive testimony to atmospheric neutrino oscillations. Not only did it show data compatible with $\nu_\mu \rightarrow \nu_\tau$ oscillation⁵, but it also highlighted the dependence of this phenomenon on the neutrino energy and the distance it had travelled.

⁴To be precise, downward events are defined by $\cos \theta \in [0.2, 1]$ and upward events by $\cos \theta \in [-1, -0.2]$.

⁵Tau neutrinos were the only ones that Super-Kamiokande could not detect, hence the deficit. The OPERA collaboration would later endeavour to detect the $\nu_\mu \rightarrow \nu_\tau$ oscillation.

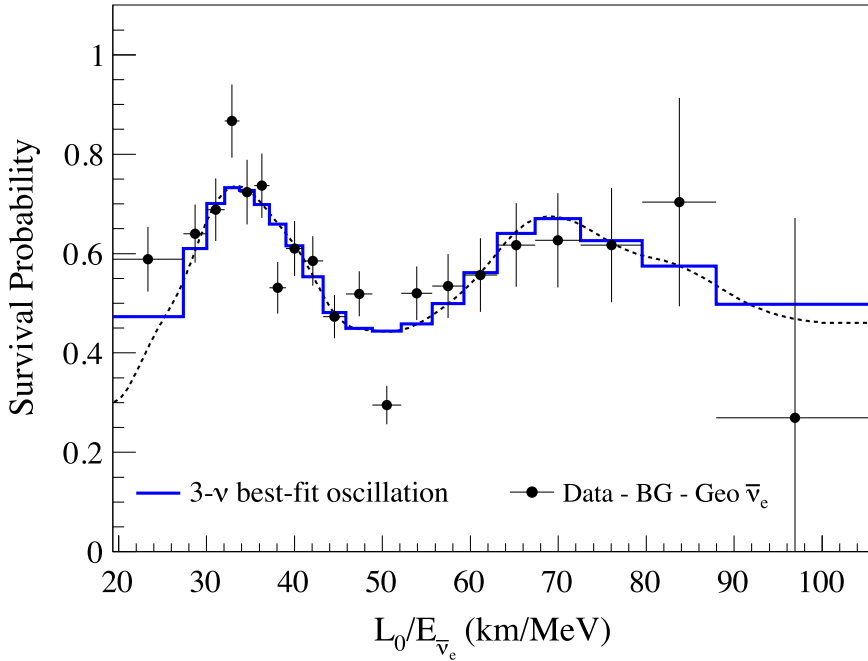


Figure 2.3 – Ratio of the background-subtracted number of $\bar{\nu}_e$'s to the expectation for no-oscillation, as a function of $L_0/E_{\bar{\nu}_e}$, with $L_0 = 180$ km the effective baseline and $E_{\bar{\nu}_e}$, the $\bar{\nu}_e$ energy. Extracted from KamLAND's data [38].

2.1.3.3 Anthropogenic neutrinos

Man-made sources do not fall short of expectations, they allowed us to discover the neutrino, and it is to them that we shall turn – in the framework of this thesis – to understand one of the last properties of neutrino oscillations.

Shortly after SNO's marvellous results, at the former Kamiokande site, the Kamioka Liquid Scintillator Anti-Neutrino Detector (KamLAND) was bent on observing oscillating $\bar{\nu}_e$'s, which were produced by the sizeable number of Japanese nuclear reactors. To characterise the $\bar{\nu}_e$'s, that had journeyed along a typical flux-weighted 180 km baseline, the detection method of choice was the inverse β -decay reaction (1.6), with which F. Reines and C. L. Cowan had raised their profiles (see 1.1.3). Unsurprisingly, in 2003, a deficit with respect to the standard expectation was observed, with a 4σ significance [36]. The unimpeachable energy-dependence of this deficit would latter be refined [37], thereby upholding it as the trademark of neutrino oscillations (at fixed distances). An up-to-date plot of this signature is to be found in Figure 2.3.

At much shorter baselines – essentially, a few hundreds of meters – the two thousand and tens have cast the limelight onto the Daya Bay, RENO (Reactor Experiment for Neutrino Oscillation), and Double Chooz reactor experiments, whose achievements we shall review later, for they all aim at precisely measuring the smallest (anti)neutrino deficit ever observed.

However discreet neutrinos can be, accelerator neutrinos are by no means bystanders.

In fact, in June 2011, the Tokai to Kamioka (T2K) collaboration provided the first positive indication of the value of the smallest deficit, with a 2.5σ significance [39]. Besides, with their energies of the order the GeV, and their baselines of a few hundreds of kilometres, experiments such as MINOS [40] tackle the same type of oscillation that affects atmospheric neutrinos. In addition, they do it with a different sensitivity, as will become obvious after we have laid the theoretical groundwork for measuring all the physical quantities that drive neutrino oscillations, in section 2.2.

2.2 Theory of neutrino oscillations

2.2.1 First draft

All the deficits and patterns observed by the previously introduced experiments can be explained in the framework of neutrino oscillations.

Although B. Pontecorvo, inspired by the kaon transitions $K^0 \rightarrow \bar{K}^0$, had speculated on the oscillation of neutral⁶ particles in 1957 [41], and thus on that of $\nu \rightarrow \bar{\nu}$ [42] – each of which possibly being a quantum superposition of other particles – it is not quite the phenomenon that has been observed over the last fifty years⁷. In 1962, Ziro Maki, Masami Nakagawa and Shoichi Sakata, in an attempt to unify all particles into a unitary scheme, put forth the quaint idea that baryons could be compound systems of leptons and a new sort of "B-matter" [43]. Stirred by the ν_μ discovery (cf. 1.2.1), they also contemplated, for the first time, that the "weak" neutrinos ν_e and ν_μ , could be a mixture of "true" neutrinos ν_1 and ν_2 , and therefore that $\nu_e \rightleftharpoons \nu_\mu$ conversions, or rather, oscillations, were possible. They postulated that both representations were related by an orthogonal transformation, and that the weak neutrinos – which should separately conserve the leptonic numbers (see 1.2.1) – were but rotated versions of the true ones⁸,

$$\begin{cases} |\nu_e\rangle &= \cos \theta |\nu_1\rangle + \sin \theta |\nu_2\rangle, \\ |\nu_\mu\rangle &= -\sin \theta |\nu_1\rangle + \cos \theta |\nu_2\rangle, \end{cases} \quad (2.16)$$

with $\theta \in [0, \pi/2]$, the angle between the states $|\nu_e\rangle$ and $|\nu_1\rangle$.

⁶B. Pontecorvo paid attention to neutral particles because he focused on particle to anti-particle transitions, which are otherwise intricate...

⁷It does relate to the search for neutrinoless double-beta decays, though.

⁸In [43], the angle is actually opposite ours, and the true neutrinos are the ones rotated by θ with respect to the weak neutrinos, but we here follow the modern convention, that will simplify later comparisons and ease the reading.

2.2.2 Mixing matrix

2.2.2.1 Two-dimensional formalism

It would, however, take more than ten years, and the vital progress made by Cabibbo in the quark sector, to make plain that the weak neutrinos do not have a definite mass [44], and that there exists mixing with what are the true mass eigenstates [45]. Accordingly, we shall henceforth call the former "flavour eigenstates", and the latter, "mass eigenstates".

Mathematically, the system (2.16) defines the coordinates of the flavour neutrinos in the mass basis, from which is derived the change of basis matrix

$$P_m^{fl} = \begin{pmatrix} \cos \theta & -\sin \theta \\ \sin \theta & \cos \theta \end{pmatrix}. \quad (2.17)$$

The P_m^{fl} matrix embodies the rotation of the mass eigenstates by an angle of θ and allows to convert back into the mass basis, the coordinates of neutrinos which are expressed in terms of the flavour eigenstates. Explicitly writing the basis as a subscript turns the counter-intuitive observation into a rule of thumb (superscripts and subscripts cancel)

$$|\nu_m\rangle = P_m^{fl} |\nu_{fl}\rangle. \quad (2.18)$$

From there, the aptly-named change of basis matrix U_{MNS} reads

$$U_{MNS} = P_m^m = (P_m^{fl})^{-1} = {}^t P_m^{fl} = \begin{pmatrix} \cos \theta & \sin \theta \\ -\sin \theta & \cos \theta \end{pmatrix}, \quad (2.19)$$

with the transpose being indicated as a pre-superscript. Consequently, the U_{MNS} matrix corresponds to a rotation by an angle $(-\theta)$ and its columns are simply the coordinates of the mass eigenstates in the flavour basis, hence partly justifying the abusive writing

$$U_{MNS} = \begin{pmatrix} U_{e1} & U_{e2} \\ U_{\mu 1} & U_{\mu 2} \end{pmatrix}. \quad (2.20)$$

The U_{MNS} matrix is the rotation we wish to apply to neutrinos in the "true" mass basis in order to get their coordinates in the flavour basis

$$|\nu_{fl}\rangle = U_{MNS} |\nu_m\rangle. \quad (2.21)$$

Any state from the mass basis reads $|\nu_m\rangle = x_1 |\nu_1\rangle + x_2 |\nu_2\rangle$, with x_1 and x_2 arbitrary complex numbers. In the mass basis, $|\nu_m\rangle$ simply reads

$$|\nu_m\rangle = \begin{pmatrix} x_1 \\ x_2 \end{pmatrix}_m. \quad (2.22)$$

Applying U_{MNS} , we obtain (x_e, x_μ) , the coordinates of this state in the flavour basis

$$|\nu_{fl}\rangle = \begin{pmatrix} x_e \\ x_\mu \end{pmatrix}_{fl} = \begin{pmatrix} \cos \theta x_1 + \sin \theta x_2 \\ -\sin \theta x_1 + \cos \theta x_2 \end{pmatrix}_{fl}. \quad (2.23)$$

2.2. THEORY OF NEUTRINO OSCILLATIONS

Taking $x_1 = 1$ and $x_2 = 0$ confirms that

$$|\nu_1\rangle = \cos \theta |\nu_e\rangle - \sin \theta |\nu_\mu\rangle. \quad (2.24)$$

The diligence of this paragraph may seem overly pedantic to the reader, but (2.24) is there to stress that U_{MNS} allows to expand the mass eigenstates into the flavour basis, and not the other way around, which is, more often than not, stated in other documents, based on an erroneous interpretation of (2.21). Such statements, in the generalisation that is to follow, usually lead to magical air-drops of stars in a crooked attempt to get the complex conjugates on the coefficients of U_{MNS} ⁹.

2.2.2.2 Three-dimensional case

Change of basis

When adding the tau neutrinos, the U_{MNS} matrix sometimes gets an additional subscript letter, hereby turning into U_{PMNS}

$$U_{PMNS} = P_{fl}^m = \begin{pmatrix} U_{e1} & U_{e2} & U_{e3} \\ U_{\mu 1} & U_{\mu 2} & U_{\mu 3} \\ U_{\tau 1} & U_{\tau 2} & U_{\tau 3} \end{pmatrix}, \quad (2.25)$$

which is a unitary matrix, and thus satisfies an equation similar to (2.19), that is

$$P_m^{fl} = (U_{PMNS})^{-1} = (U_{PMNS})^\dagger, \quad (2.26)$$

where the \dagger denotes the Hermitian transpose. Accordingly

$$P_m^{fl} = \begin{pmatrix} {U_{e1}}^* & {U_{\mu 1}}^* & {U_{\tau 1}}^* \\ {U_{e2}}^* & {U_{\mu 2}}^* & {U_{\tau 2}}^* \\ {U_{e3}}^* & {U_{\mu 3}}^* & {U_{\tau 3}}^* \end{pmatrix}, \quad (2.27)$$

and any flavour eigenstate $|\nu_\alpha\rangle$ where $\alpha \in \{e, \mu, \tau\}$, represented by a 1 at the α -th line of a column vector in the flavour basis, has the following coordinates in the mass basis

$$|\nu_\alpha\rangle = \begin{pmatrix} {U_{\alpha 1}}^* \\ {U_{\alpha 2}}^* \\ {U_{\alpha 3}}^* \end{pmatrix}_m. \quad (2.28)$$

In terms of states, we have for all $\alpha \in \{e, \mu, \tau\}$,

$$|\nu_\alpha\rangle = \sum_{k=1}^3 {U_{\alpha k}}^* |\nu_k\rangle = \sum_{k=1}^3 U_{k\alpha}^{-1} |\nu_k\rangle = \sum_{k=1}^3 (P_m^{fl})_{k\alpha} |\nu_k\rangle, \quad (2.29)$$

hereby corroborating the first-class role of P_m^{fl} , which is often improperly peddled as U_{PMNS} .

⁹When tackling this issue the proper way, that is, starting from quantum fields, one gets complex conjugates from the creation operators for particles, as opposed to antiparticles, the former bearing a "dagger".

Parametrisation

Let us express the U_{PMNS} matrix in the case of N neutrino flavours and N mass eigenstates, with $N > 1$. Each eigenvalue λ , of a unitary matrix U , has modulus $|\lambda| = 1$, thus, there exists θ such that $\lambda = \exp(i\theta)$. By diagonalising the matrix, it is easy to see that it can be written as the exponential of a Hermitian matrix H so that

$$U = \exp(iH). \quad (2.30)$$

Since $H = H^\dagger$, Hermitian matrices have N diagonal real terms, and $N(N-1)/2$ off-diagonal independent complex terms, thereby amounting to a total of N^2 independent real coefficients. Likewise, orthogonal matrices O can be written

$$O = \exp(A), \quad (2.31)$$

where A is antisymmetric and verifies ${}^t A = -A$, leaving room for

$$N_\theta = \frac{N(N-1)}{2} \quad (2.32)$$

real coefficients, or angles. Consequently, of the N^2 real coefficients that parametrise a unitary matrix, there remains

$$N_\delta = \frac{N(N+1)}{2} \quad (2.33)$$

phases, which cannot be expressed as angles. Nevertheless, $2N-1$ of these phases are already free parameters of the lepton fields¹⁰, which leaves

$$N_\delta^{free} = \frac{N(N+1)}{2} - (2N-1) = \frac{(N-1)(N-2)}{2} \quad (2.34)$$

free phases in the U_{PMNS} matrix.

Plugging $N = 3$ in (2.32) and (2.34), provides us with three mixing angles, which we baptise θ_{12} , θ_{13} , θ_{23} , and one phase δ . Abiding by the usual parametrisation (see [46]), for Dirac neutrinos, we can write

$$U_{PMNS} = \begin{pmatrix} 1 & 0 & 0 \\ 0 & c_{23} & s_{23} \\ 0 & -s_{23} & c_{23} \end{pmatrix} \begin{pmatrix} c_{13} & 0 & s_{13}e^{-i\delta} \\ 0 & 1 & 0 \\ -s_{13}e^{i\delta} & 0 & c_{13} \end{pmatrix} \begin{pmatrix} c_{12} & s_{12} & 0 \\ -s_{12} & c_{12} & 0 \\ 0 & 0 & 1 \end{pmatrix}, \quad (2.35)$$

with $c_{ij} = \cos(\theta_{ij})$, $s_{ij} = \sin(\theta_{ij})$. When multiplying all matrices out, we find

$$U_{PMNS} = \begin{pmatrix} c_{12}c_{13} & s_{12}c_{13} & s_{13}e^{-i\delta} \\ -s_{12}c_{23} - c_{12}s_{23}s_{13}e^{i\delta} & c_{12}c_{23} - s_{12}s_{23}s_{13}e^{i\delta} & s_{23}c_{13} \\ s_{12}c_{23} - c_{12}c_{23}s_{13}e^{i\delta} & -c_{12}s_{23} - s_{12}c_{23}s_{13}e^{i\delta} & c_{23}c_{13} \end{pmatrix}. \quad (2.36)$$

Solar experiments deal with parameters related to $|U_{e2}/U_{e1}| = \tan(\theta_{12})$ and atmospheric experiments, with $|U_{\mu 3}/U_{\tau 3}| = \tan(\theta_{13})$. In the meantime, reactor experiments, such as Double Chooz, are particularly interested in $|U_{e3}| = \sin(\theta_{13})$, as the title of this thesis hints at.

¹⁰For Dirac neutrinos, global $U(1)$ gauge transformations are indeed allowed for e, μ, τ and ν_e, ν_μ, ν_τ .

2.2.3 Quantum-mechanical approach

2.2.3.1 Plane wave derivation

If truth be told, all this does not tell us how to experimentally extract the aforementioned parameters. In fact, all the experiments we have reviewed in section 2.1 involve neutrino production of a certain flavour, may it be in the sun as ν_e 's, in the atmosphere as ν_e 's, $\overline{\nu}_\mu$'s $\overline{\nu}_e$'s and ν_μ 's, or in nuclear reactors, as $\overline{\nu}_e$'s. They also imply propagation from the production area to the detector, and eventually, detection, by charged or neutral currents. As 2.2.2 recommends, all these operations imply thoughtful change of coordinates, which is precisely how the U_{PMNS} coefficients – that we strive to measure – end up in the equations.

We hereby present the simpler quantum-mechanical derivation of the oscillation probabilities in vacuum, an approach based on quantum field theory can be studied in [47]. To do so, we start with a flavour eigenstate $|\nu_\alpha\rangle$ with $\alpha \in \{e, \mu, \tau\}$, produced at the space-time origin

$$|\nu_\alpha(0)\rangle = |\nu_\alpha\rangle. \quad (2.37)$$

In order to easily propagate this state to another location, let us first expand it with respect to the mass eigenstates $(\nu_k)_{k \in \llbracket 1, 3 \rrbracket}$. As underscored by (2.29), we obtain

$$|\nu_\alpha(0)\rangle = \sum_{k=1}^3 U_{k\alpha}^{-1} |\nu_k\rangle = \sum_{k=1}^3 U_{\alpha k}^* |\nu_k\rangle. \quad (2.38)$$

Assuming that the mass eigenstates follow the time-dependent Schrödinger equation with no potentials – as is the case in vacuum – at a different point x in space-time, for all $k \in \llbracket 1, 3 \rrbracket$, we have

$$|\nu_k(x)\rangle = e^{-ip_k \cdot x} |\nu_k\rangle, \quad (2.39)$$

where p_k is the four-momentum of the k -th state. Thus, the state $|\nu_\alpha(x)\rangle$ evolves as

$$|\nu_\alpha(x)\rangle = \sum_{k=1}^3 U_{\alpha k}^* e^{-ip_k \cdot x} |\nu_k\rangle. \quad (2.40)$$

Detecting $|\nu_\alpha(x)\rangle$ amounts to projecting it on a flavour eigenstate $|\nu_\beta\rangle$ with $\beta \in \{e, \mu, \tau\}$. For this reason, it is suitable to expand the $|\nu_k\rangle$'s back to the flavour basis, which, for once, does rely on U_{PMNS} , from which we can directly read the column vectors introduced in (2.25). When doing so, we find

$$|\nu_\alpha(x)\rangle = \sum_{k=1}^3 \sum_{\gamma=e,\tau,\mu} U_{\alpha k}^* U_{\gamma k} e^{-ip_k \cdot x} |\nu_\gamma\rangle. \quad (2.41)$$

Since the flavour eigenstates form an orthonormal set, the probability for a neutrino of a

given flavour α , produced at origin, to be detected with a β flavour at x is

$$\begin{aligned} P_{\nu_\alpha \rightarrow \nu_\beta} &= |\langle \nu_\beta | \nu_\alpha(x) \rangle|^2 \\ &= \left| \sum_{k=1}^3 U_{\alpha k}^* U_{\beta k} e^{-i p_k \cdot x} \right|^2 \\ &= \sum_{k=1}^3 \sum_{j=1}^3 U_{\alpha k}^* U_{\beta k} U_{\alpha j} U_{\beta j}^* e^{-i(p_k - p_j) \cdot x}. \end{aligned} \quad (2.42)$$

It is worthwhile noting that for antineutrinos, the expansion of the flavour eigenstates into the mass basis proceeds through U_{PMNS} directly, which would exchange the conjugate terms in (2.42).

2.2.3.2 Ultra-relativistic approximation

A few dodgy assumptions are now needed to simplify further (2.42) and derive its usual form for neutrino experiments. The masses of the neutrinos are very small compared to the energies at which they are detected, in a nutshell, neutrinos are ultra-relativistic particles¹¹. In natural units, this implies that $t \simeq \|\vec{x}\| = L$, where L is the distance between the neutrino source and the detector (on whose direction the three-momenta \vec{p}_k 's are taken to be aligned). Consequently, the phases can be approximated by

$$(p_k - p_j) \cdot x \simeq [(E_k - \|\vec{p}_k\|) - (E_j - \|\vec{p}_j\|)] L. \quad (2.43)$$

Carrying on with the ultra-relativistic assumption, we assume that the energy E , given by the kinematics of the production process neglecting neutrino masses, verifies, for all $k \in \llbracket 1, 3 \rrbracket$

$$E_k - \|\vec{p}_k\| = \frac{m_k^2}{E_k + \|\vec{p}_k\|} \simeq \frac{m_k^2}{2E}, \quad (2.44)$$

so that we can write

$$(p_k - p_j) \cdot x \simeq \frac{\Delta m_{kj}^2}{2E} L, \quad (2.45)$$

where $\Delta m_{kj}^2 = m_k^2 - m_j^2$. Inserting (2.45) into (2.42) eventually leads to the probability to detect a neutrino oscillation at a distance L from a source which produces them with a (kinetic) energy E

$$P_{\nu_\alpha \rightarrow \nu_\beta}(L, E) = \sum_{k=1}^3 \sum_{j=1}^3 U_{\alpha k}^* U_{\beta k} U_{\alpha j} U_{\beta j}^* e^{-i \frac{\Delta m_{kj}^2}{2E} L}. \quad (2.46)$$

¹¹We are treating relativistic particles as plane waves, we could hardly do with less sense regarding that plane waves are everywhere but nowhere, nevertheless, imposing coherent contributions of wave packets yields identical results, see [48] for discussions.

2.2.3.3 Oscillation probabilities with trigonometric functions

We can expand (2.46) into a more usable form that has only trigonometric functions. For each space-time position x , regardless of any relativistic approximation, (2.42) and (2.46) bring out a Hermitian matrix in $(k, j) \in \llbracket 1, 3 \rrbracket^2$, whose coefficients read

$$h_{kj} = U_{\alpha k}^* U_{\beta k} U_{\alpha j} U_{\beta j}^* e^{-i(p_k - p_j) \cdot x}. \quad (2.47)$$

Evidently, these satisfy $h_{kj} = h_{jk}^*$. It is apposite to take advantage of the Hermitian symmetry and split the integral into diagonal and off-diagonal terms

$$\begin{aligned} \sum_{k=1}^3 \sum_{j=1}^3 h_{kj} &= \sum_{k=1}^3 h_{kk} + \sum_{k=1}^3 \sum_{j=1}^{k-1} h_{kj} + \sum_{k=1}^3 \sum_{j=k+1}^3 h_{kj} \\ &= \sum_{k=1}^3 h_{kk} + \sum_{k=2}^3 \sum_{j=1}^{k-1} h_{kj} + \sum_{k=1}^2 \sum_{j=k+1}^3 h_{kj}. \end{aligned} \quad (2.48)$$

Up to a conjugate, the last term is identical to the second one, as a result

$$\sum_{k=1}^3 \sum_{j=1}^3 h_{kj} = \sum_{k=1}^3 h_{kk} + 2 \sum_{k=2}^3 \sum_{j=1}^{k-1} \Re(h_{kj}), \quad (2.49)$$

where \Re denotes the real part. Along these lines,

$$\begin{aligned} P_{\nu_\alpha \rightarrow \nu_\beta}(L, E) &= \sum_{k=1}^3 |U_{\alpha k}|^2 |U_{\beta k}|^2 + 2 \sum_{k=2}^3 \sum_{j=1}^{k-1} \Re \left(U_{\alpha k}^* U_{\beta k} U_{\alpha j} U_{\beta j}^* e^{-i \frac{\Delta m_{kj}^2 L}{2E}} \right) \\ &= \sum_{k=1}^3 |U_{\alpha k}|^2 |U_{\beta k}|^2 + 2 \sum_{k=2}^3 \sum_{j=1}^{k-1} \cos \left(\frac{\Delta m_{kj}^2 L}{2E} \right) \Re (U_{\alpha k}^* U_{\beta k} U_{\alpha j} U_{\beta j}^*) \\ &\quad + 2 \sum_{k=2}^3 \sum_{j=1}^{k-1} \sin \left(\frac{\Delta m_{kj}^2 L}{2E} \right) \Im (U_{\alpha k}^* U_{\beta k} U_{\alpha j} U_{\beta j}^*), \end{aligned} \quad (2.50)$$

since $\exp \left(-i \frac{\Delta m_{kj}^2 L}{2E} \right) = \cos \left(\frac{\Delta m_{kj}^2 L}{2E} \right) - i \sin \left(\frac{\Delta m_{kj}^2 L}{2E} \right)$. The unitarity of U_{PMNS} also implies that

$$\left(\sum_{k=1}^3 U_{\alpha k} U_{k\beta}^\dagger \right)^2 = \delta_{\alpha\beta}. \quad (2.51)$$

Using the same property that yielded (2.49), we obtain

$$\sum_{k=1}^3 |U_{\alpha k}|^2 |U_{\beta k}|^2 = \delta_{\alpha\beta} - 2 \sum_{k=2}^3 \sum_{j=1}^{k-1} \Re (U_{\alpha k}^* U_{\beta k} U_{\alpha j} U_{\beta j}^*). \quad (2.52)$$

Substituting (2.52) into (2.50), we conclude that

$$\begin{aligned} P_{\nu_\alpha \rightarrow \nu_\beta}(L, E) &= \delta_{\alpha\beta} - 4 \sum_{k=2}^3 \sum_{j=1}^{k-1} \sin^2 \left(\frac{\Delta m_{kj}^2 L}{4E} \right) \Re (U_{\alpha k}^* U_{\beta k} U_{\alpha j} U_{\beta j}^*) \\ &\quad + 2 \sum_{k=2}^3 \sum_{j=1}^{k-1} \sin \left(\frac{\Delta m_{kj}^2 L}{2E} \right) \Im (U_{\alpha k}^* U_{\beta k} U_{\alpha j} U_{\beta j}^*). \end{aligned} \quad (2.53)$$

2.2.3.4 Survival probability

Nuclear power plants, in which we are most interested, are actually generators of antineutrinos. One could go back to 2.2.3.1 and read the comments there that concern antineutrinos to derive the antineutrino version of (2.53), but we can also use some ingenuity and recall that CP transforms left-handed neutrinos into right-handed antineutrinos (cf. 1.2.2), the time operator T , on the other hand, essentially changes the direction of the arrow in the probability $P_{\nu_\alpha \rightarrow \nu_\beta}$. To put it differently,

$$P_{\bar{\nu}_\alpha \rightarrow \bar{\nu}_\beta} = P_{\nu_\beta \rightarrow \nu_\alpha} \quad (2.54)$$

as long as CPT holds, and it does, so far. Recalling that the real part of a complex number is unaffected by conjugation, and that the imaginary part takes a minus sign, we can explicitly write

$$\begin{aligned} P_{\bar{\nu}_\alpha \rightarrow \bar{\nu}_\beta}(L, E) = & \delta_{\alpha\beta} - 4 \sum_{k=2}^3 \sum_{j=1}^{k-1} \sin^2 \left(\frac{\Delta m_{kj}^2 L}{4E} \right) \Re (U_{\alpha k}^* U_{\beta k} U_{\alpha j} U_{\beta j}^*) \\ & - 2 \sum_{k=2}^3 \sum_{j=1}^{k-1} \sin \left(\frac{\Delta m_{kj}^2 L}{2E} \right) \Im (U_{\alpha k}^* U_{\beta k} U_{\alpha j} U_{\beta j}^*). \end{aligned} \quad (2.55)$$

The survival probability, which determines the chances to project the incoming neutrino back to the flavour state $|\nu_\alpha\rangle$ with which one started, is even simpler than (2.55)

$$P_{\bar{\nu}_\alpha \rightarrow \bar{\nu}_\alpha}(L, E) = P_{\nu_\alpha \rightarrow \nu_\alpha}(L, E) = 1 - 4 \sum_{k=2}^3 \sum_{j=1}^{k-1} |U_{\alpha k}|^2 |U_{\alpha j}|^2 \sin^2 \left(\frac{\Delta m_{kj}^2 L}{4E} \right). \quad (2.56)$$

2.3 Parameters of the model

2.3.1 Neutrino masses

2.3.1.1 Individual masses

On top of a non-diagonal mixing matrix, it should now be clearer – with the help of section 2.2 – why neutrino oscillations demand the neutral leptons to have mass. All the fuss about physics beyond the Standard Model comes from the neutrino masses, whose simplest experimental signature is neutrino oscillations. To be fair, at least two of the mass eigenstates $(\nu_k)_{k \in \llbracket 1, 3 \rrbracket}$ should have a non-vanishing mass, since the oscillation probabilities boil down to the squared mass differences introduced in (2.45). The individual masses are indeed difficult to access experimentally, and direct measurements of the electron neutrino mass – which is but a U_{PMNS} -weighted average of the mass eigenvalues $(m_k)_{k \in \llbracket 1, 3 \rrbracket}$ – relying on the endpoint of the β -decay of tritium, have only been able to set an upper-limit [49]

$$m_{\bar{\nu}_e} = \sqrt{\langle \bar{\nu}_e | M^2 | \bar{\nu}_e \rangle} = \sqrt{\sum_{k=1}^3 |U_{ek}|^2 m_k^2} < 2.05 \text{ eV} \quad (95\% \text{CL}), \quad (2.57)$$

where M designs the mass operator, which is diagonal in the mass basis. Other model-dependent limits, coming from cosmology, have set more stringent limits on the sum of the mass eigenvalues themselves [50]

$$\sum_{k=1}^3 m_k < 0.136 \text{ eV} \quad (95\% \text{CL}). \quad (2.58)$$

2.3.1.2 Squared mass differences

As is apparent from (2.53), the frequencies that drive the probability to detect one flavour or another, as a function of L/E , are explicitly related to the squared mass differences, and are responsible for the pattern from Figure 2.3. There are various regimes, determined by the energy of the neutrino source, the location of the detector with respect to the source, and of course, by the distribution of the squared mass differences. Fortunately, the latter are well-separated and allow experiments to focus on one particular set of values. Echoing back to our comments from 2.1.3.3, that is precisely because they can adjust relatively well the L/E ratio – hence overshadowing irrelevant terms in the oscillation probabilities – that man-made neutrinos particularly shine when it comes to estimating certain parameters.

From solar neutrinos¹², we have learnt that [51]

$$\Delta m_{21}^2 = (7.53 \pm 0.18) \times 10^{-5} \text{ eV}^2. \quad (2.59)$$

On the other hand, atmospheric neutrinos¹³ have us wavering between the two conflicting values that follow [51]

$$\Delta m_{32}^2 = (2.44 \pm 0.06) \times 10^{-3} \text{ eV}^2 \quad (2.60)$$

$$\text{OR} \quad \Delta m_{32}^2 = - (2.49 \pm 0.06) \times 10^{-3} \text{ eV}^2. \quad (2.61)$$

How come we seem to only have knowledge about the absolute value $|\Delta m_{32}^2|$, which cannot be distinguished from $|\Delta m_{31}^2|$? Why are there two different numbers for Δm_{32}^2 ? As it happens, we do not know yet if the two close mass eigenstates, ν_1 and ν_2 , are much lighter than ν_3 , or if there actually are two "heavy" neutrinos out there. The first situation, in which $\Delta m_{32}^2 > 0$, is referred to as the "normal mass hierarchy", the second one corresponds to $\Delta m_{32}^2 < 0$ and goes by the name of "inverted mass hierarchy". To get a better grasp of these ambiguities, we must look for bare sines in (2.53) and (2.55), which are the sole terms that can tell us about the signs of the squared mass differences. From (2.56), it is clear that no such information can effortlessly come from the study of neutrino survival, for one would have to endeavour to see sub-leading order differences between Δm_{32}^2 and Δm_{31}^2 ¹⁴. Unfortunately, in apparition

¹²KamLAND is effectively looking at the solar regime although the lightweight leptons it observes come from nuclear reactors.

¹³Accelerator neutrinos, observed by MINOS and K2K, shed light on the same parameters as atmospheric neutrinos.

¹⁴By and large, the JUNO experiment will actually try to understand if $|\Delta m_{32}^2| > |\Delta m_{31}^2|$, which would correspond to a normal ordering.

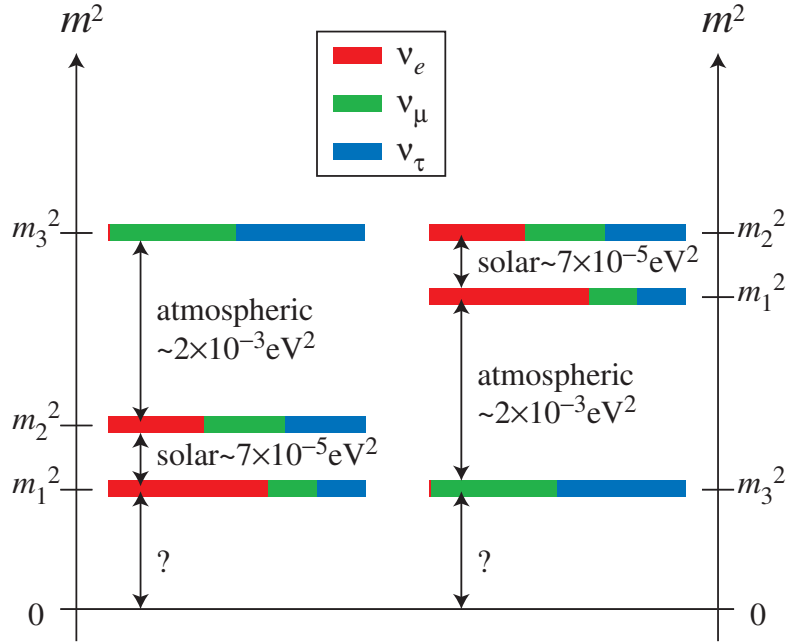


Figure 2.4 – Visual summary of the knowledge about neutrino oscillations. On the left-hand side, the normal mass hierarchy is assumed, on the right, the inverted ordering is presented. The colourful bars indicate the components of the mass eigenstates in the flavour basis. For instance, the state of mass m_1 has its largest component along $|\nu_e\rangle$ whereas $|\nu_3\rangle$ has barely any weight along it, on account of the tininess of θ_{13} . Figure taken from [53].

experiments, which answer for $P_{\nu_\alpha \rightarrow \nu_\beta}$ with $\alpha \neq \beta$, the set of model parameters is such that the bare sine terms are also second order corrections. The different behaviour of neutrinos and antineutrinos in matter can, however, help to disentangle the two mass hierarchies [52]. While on the subject, that it is precisely due to the considerable matter effect in the sun that the ordering $m_2 > m_1$ has been resolved.

A visual representation of the knowledge about neutrino masses can be found in Figure 2.4, it presents the two possible mass hierarchies and serves as an appetiser for the next sub-section, which tackles the coefficients of U_{PMNS} .

2.3.2 Matrix coefficients

2.3.2.1 Large mixing angles

The squared mass differences appear in the sines of the oscillation formula (2.53), and accordingly, determine the frequency with which the values of the probabilities are repeated when moving along a L/E axis. On the other hand, the amplitude of the oscillations is fixed by the U_{PMNS} matrix coefficients. As reviewed in 2.2.2.2, the mixing matrix consists of three angles of rotation $\theta_{12}, \theta_{13}, \theta_{23}$ and one phase δ . Nonetheless, the coefficients of the

2.3. PARAMETERS OF THE MODEL

matrix remain to be predicted by any theory, and we must rely on experiments to set their values¹⁵. For the solar sector, these experiments have observed [51]

$$\sin^2(\theta_{12}) = 0.304 \pm 0.014, \quad (2.62)$$

and for the atmospheric angle, we have [51]

$$\sin^2(\theta_{23}) = 0.514 \pm 0.056 \quad (2.63)$$

$$\text{OR} \quad \sin^2(\theta_{23}) = 0.511 \pm 0.055, \quad (2.64)$$

where (2.64) is the estimation in the case of an inverted mass hierarchy.

2.3.2.2 Minute mixing angle

With regards to the remaining mixing angle θ_{13} , it has proven to be the most challenging to quantify and it remained unmeasured until just a few years ago. In the pursuit of its measurement, two types of experiments have been undertaken: accelerator experiments and reactor experiments.

The former, such as T2K and MINOS, are relying on ν_e appearance in a ν_μ beam. To put it differently, these experiments are measuring $P_{\nu_\mu \rightarrow \nu_e}$, which involves the real and imaginary parts of the terms $U_{\mu k}^* U_{ek} U_{\mu j} U_{ej}^*$ for $2 \leq k \leq 3$ and $1 \leq j \leq k-1$. Thus, these terms are dependent on the unknown δ phase, that will be presented more in-depth in 2.3.2.3. Besides, as underlined in 2.3.1.2, there are second order corrections related to the mass hierarchy in the apparition formula¹⁶.

On the contrary, insofar as the survival formula (2.56) bears only moduli, disappearance experiments are utterly agnostic as to whether the U_{PMNS} matrix is complex or purely real, i.e. they are independent of whether $\delta \neq 0$ or $\delta = 0$. Moreover, inasmuch as there are only squared sines in (2.56), they are, for the most part, free from assumptions on the mass hierarchy provided that $\Delta m_{32}^2 \simeq \Delta m_{31}^2$. Therefore, it is scarcely surprising that reactor experiments such as Daya Bay, RENO, and Double Chooz, have set the most stringent bounds on the value of $\sin^2(\theta_{13})$.

Electron antineutrino survival in the vicinity of a nuclear power plant

Let us explicitly write the survival probability for the $\bar{\nu}_e$'s produced in nuclear reactors, and detected a few hundreds of meters farther, via inverse β -decay (1.6). Expanding (2.56), we

¹⁵In that regard, the neutrino masses are scarcely different since they require fine-tuned Yukawa couplings.

¹⁶Let us emphasise again that T2K and MINOS, on top of looking for ν_e appearance, are set on measuring θ_{23} and Δm_{32}^2 by ν_μ disappearance and think anyhow bigger than reactor experiments.

get

$$P_{\bar{\nu}_e \rightarrow \bar{\nu}_e}(L, E) = 1 - 4|U_{e2}|^2|U_{e1}|^2 \sin^2 \left(\frac{\Delta m_{21}^2 L}{4E} \right) - 4|U_{e3}|^2|U_{e1}|^2 \sin^2 \left(\frac{\Delta m_{31}^2 L}{4E} \right) - 4|U_{e3}|^2|U_{e2}|^2 \sin^2 \left(\frac{\Delta m_{32}^2 L}{4E} \right). \quad (2.65)$$

Recalling that

$$|U_{e1}|^2 = \cos^2(\theta_{12}) \cos^2(\theta_{13}) \simeq \cos^2(\theta_{12}) = 1 - \sin^2(\theta_{12}) \quad (2.66)$$

$$|U_{e2}|^2 = \sin^2(\theta_{12}) \cos^2(\theta_{13}) \simeq \sin^2(\theta_{12}) \quad (2.67)$$

$$|U_{e3}|^2 = \sin^2(\theta_{13}), \quad (2.68)$$

and in light of the value from (2.62), it may seem as though the last two terms in (2.65) are negligible compared to the first. That would be too hasty a judgement, for we must first discuss the value of the phase. As such, rewriting back the c^2 next to each mass, with c being the speed of light, the phases are in $\text{MeV} \cdot \text{fm}$ or any equivalent unit. To cut the matter short, the phases are missing $\hbar c$, with \hbar the reduced Planck constant, and read in conventional units

$$\frac{\Delta m^2 c^4 L}{4\hbar c E} \simeq 1.27 \times 10^6 \text{ eV}^{-1} \text{m}^{-1} \frac{\Delta m^2 c^4 L}{E}. \quad (2.69)$$

In reactor experiments looking for θ_{13} , typically $E = 3 \text{ MeV}$ and $L = 10^3 \text{ m}$, so we may benefit from writing

$$\frac{\Delta m^2 c^4 L}{4\hbar c E} \simeq 4.2 \times 10^2 \text{ eV}^{-2} \Delta m^2 c^4. \quad (2.70)$$

Considering the measurements from 2.3.1.2, it is plain to see that the first sine falls in the approximation $\sin^2 x \sim x^2$ with $x \simeq 3 \times 10^{-2}$ and is consequently three orders of magnitude smaller than the last two sines, whose argument is around 1. All things considered, in our case, we have

$$P_{\bar{\nu}_e \rightarrow \bar{\nu}_e}(L, E) \simeq 1 - \sin^2(2\theta_{13}) \left[\cos^2(\theta_{12}) \sin^2 \left(\frac{\Delta m_{31}^2 L}{4E} \right) + \sin^2(\theta_{12}) \sin^2 \left(\frac{\Delta m_{32}^2 L}{4E} \right) \right], \quad (2.71)$$

since $4 \sin^2(\theta_{13}) \cos^2(\theta_{13}) = \sin^2(2\theta_{13})$. To shrink (2.71) further down, we consider that $\Delta m_{32}^2 \simeq \Delta m_{31}^2$. It follows that the oscillation probability relevant for moderately short baseline reactor experiments is well-approximated by

$$P_{\bar{\nu}_e \rightarrow \bar{\nu}_e}(L, E) \simeq 1 - \sin^2(2\theta_{13}) \sin^2 \left(\frac{\Delta m_{31}^2 L}{4E} \right). \quad (2.72)$$

In accordance, a detector located 1 km away from a nuclear power plant must show signs of an energy-dependent deficit in the neutrino spectrum it observes, as epitomised by Figure 2.5.

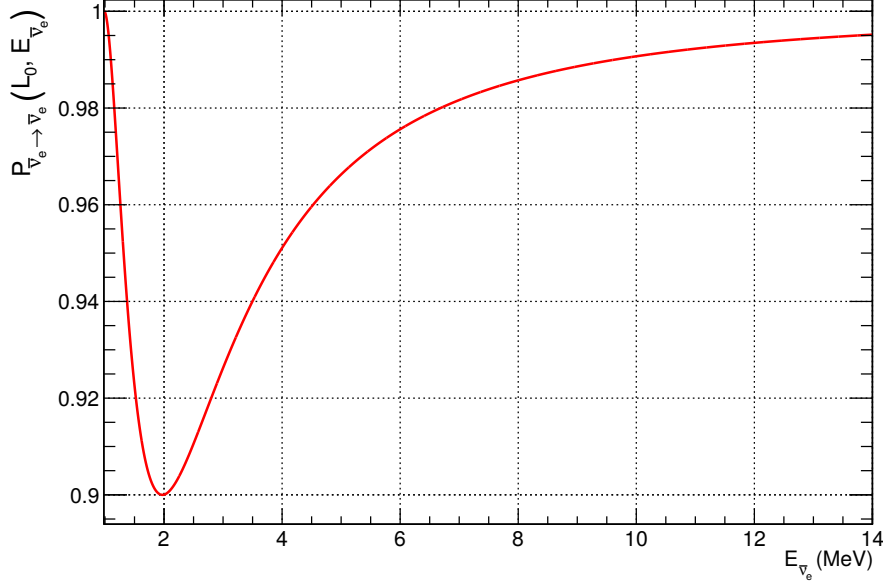


Figure 2.5 – Electron antineutrino survival probability $E_{\bar{\nu}_e} \rightarrow P_{\bar{\nu}_e \rightarrow \bar{\nu}_e}(L_0, E_{\bar{\nu}_e})$ at a distance $L_0 = 1$ km from the source. The kinetic energy of the antineutrino is designated by $E_{\bar{\nu}_e}$. The textbook case $\sin^2(2\theta_{13}) = 0.1$ is assumed.

Experimental values

In spite of the robustness of (2.72), the CHOOZ experiment – located on the current "far site" of Double Chooz (more details will follow in Chapter 3) – could but set a lower limit on the smallness of θ_{13} . Indeed, mostly plagued by liquid scintillator degradation and accidental background from several origins, at the turn of the twenty-first century, CHOOZ reported $\sin^2(2\theta_{13}) < 0.17$ (90%CL) [54].

Considerably improving the detector design used by CHOOZ, the Double Chooz collaboration showed the first indication of $\bar{\nu}_e$ disappearance in January 2012 [55], reporting $\sin^2(2\theta_{13}) = 0.086 \pm 0.041(\text{sys.}) \pm 0.030(\text{stat.})$. Notwithstanding the excellence of the Double Chooz analysis, the irrefutable evidence came from the China-based Daya Bay experiment, a few months later. In April 2012, by means of two experimental halls near Hong Kong, at distinct flux-weighted distances from the nuclear cores $L_n \simeq 500$ m and $L_f \simeq 1600$ m, the Daya Bay collaboration indeed issued [56]

$$\sin^2(2\theta_{13}) = 0.092 \pm 0.016(\text{sys.}) \pm 0.05(\text{stat.}). \quad (2.73)$$

Comparing the spectra from the detectors of the "near hall" (at which the survival probability $P_{\bar{\nu}_e \rightarrow \bar{\nu}_e}(L_n, E) \simeq 1$ for all E) to that of the "far hall" (located where the survival probability $P_{\bar{\nu}_e \rightarrow \bar{\nu}_e}(L_f, 3 \text{ MeV}) < 1$), they obtained Figure 2.6, which bears gratifying resemblance¹⁷ to

¹⁷Daya Bay's far hall actually corresponds to $L_f \simeq 1.6$ km $\neq 1$ km so the oscillation maximum is expected at $E_{\bar{\nu}_e} \simeq 3.2$ MeV. And yet, Figure 2.6 uses the prompt energy, which is about 0.8 MeV lower than $E_{\bar{\nu}_e}$, thus, it is hardly surprising that both curves look alike.

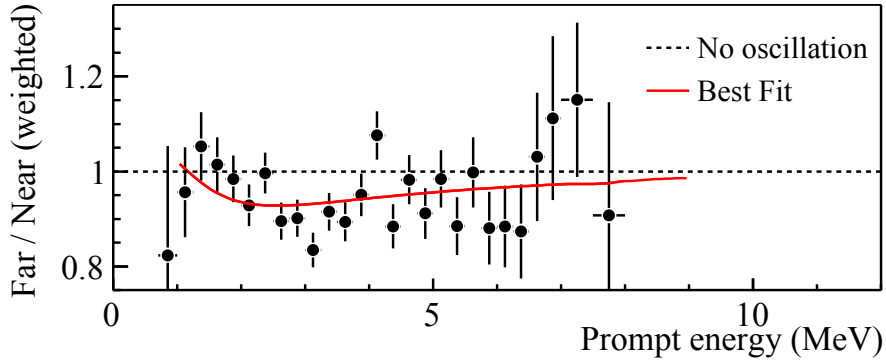


Figure 2.6 – Ratio of the far and near hall Daya Bay spectra. To all intents, the near hall spectrum is a no-oscillation prediction. The solid curve is the best-fit solution with $\sin^2(2\theta_{13}) = 0.092$, obtained from a so-called rate-only analysis, which integrates the deficit over all energies. Figure extracted from [56].

Figure 2.5. Such a differential measurement, using a "near" and a "far site", is actually the key to great accuracy. This method was first advocated by Double Chooz, at the end of the year 2002, to cancel the systematic errors originating from the prediction of the reactor spectra and to dwarf the detector-related uncertainties [57].

It is worthwhile noticing that the size of the deficit along the energy axis is driven by the phase $\Delta m_{31}^2 L / 4E$. In 2015, taking advantage of more statistics, Daya Bay thus provided an interesting measurement of m_{31}^2 ¹⁸ [58].

The Korean RENO experiment confirmed Daya Bay's θ_{13} value shortly after, in May 2012, with a comparable 4.9σ significance [59]. Although Double Chooz latest's paper [60], uses only the "far" experimental site, and exhibits a lower 3σ significance than its competitors, with $\sin^2(2\theta_{13}) = 0.090^{+0.032}_{-0.029}$, the collaboration has not kept idle hands. Not only did it build its near detector, which is put to good use in this thesis, but it also developed an unprecedented understanding of its detectors, as we shall explain in Chapter 6.

A best-fit from global analyses published up to 2015 yields [51]

$$\sin^2(2\theta_{13}) = 0.085 \pm 0.050 \quad (2.74)$$

$$\sin^2(\theta_{13}) = (2.19 \pm 0.12) \times 10^{-2}. \quad (2.75)$$

2.3.2.3 CP violation phase

To this day, the most enigmatic parameter is unmistakably the CP violation phase δ . It is called that way because if it were zero, the imaginary parts would be but nought in the

¹⁸Actually, access to $\Delta m_{ee}^2 \simeq m_{31}^2 \simeq m_{32}^2$ – which can effortlessly be defined from the square bracket in (2.71) – is offered by electron antineutrino survival.

2.3. PARAMETERS OF THE MODEL

oscillation probabilities, and the difference between (2.53) and (2.55)

$$\left(P_{\nu_\alpha \rightarrow \nu_\beta} - P_{\bar{\nu}_\alpha \rightarrow \bar{\nu}_\beta} \right) (L, E) = 4 \sum_{k=2}^3 \sum_{j=1}^{k-1} \sin \left(\frac{\Delta m_{kj}^2 L}{2E} \right) \mathfrak{Im} (U_{\alpha k}^* U_{\beta k} U_{\alpha j} U_{\beta j}^*) . \quad (2.76)$$

would vanish identically. Put another way, should $\delta = 0$, the behaviour of neutrinos and antineutrinos would be identical, and there would be no CP violation indications coming from oscillation experiments. Understanding CP violation in the neutrino sector would fill a piece in the leptogenesis puzzle, and enlighten us as to why our universe is mostly made of electrons, and not of positrons, which is a bit akin to understanding why there are so few left-handed persons in our societies¹⁹.

As is obvious in (2.36), θ_{13} has no ordinary position in the U_{PMNS} matrix. In fact, the mixing matrix has been parametrised in such a way that the smallest mixing angle is in front of the CP violation phase [46]. The smaller θ_{13} , the more difficult δ is to measure. Nevertheless, the values from (2.75) are actually large, and certainly not much smaller than CHOOZ's limit. Consequently, the very same accelerator experiments that are sensitive to θ_{13} , but hindered by corrections related to the unknown mass hierarchy and the δ value, may use the input from reactor experiments to better assess and constrain these corrections. With encouraging results already published at the beginning of the current year, NO ν A swells the list of experiments looking at ν_e appearance in a ν_μ beam [61]. Using a classical Likelihood event selector, they disfavour $0.1\pi < \delta < 0.5\pi$ for the inverted mass hierarchy at 90% CL whereas a new-fangled Library Event Matching classifier provides much bolder results, disfavouring all δ values in the case of an inverted ordering, and in this manner, the inverted mass hierarchy altogether (see Figure 2.7).

Of course, all these results are dependent on the value of θ_{13} , which is precisely the reason why the inputs handed over to these new undertakings must be cross-checked by several experiments. Beyond the shadow of a doubt, both the provided central values and the errors are of paramount importance.

¹⁹ Although shooting footballs with the left foot, as well as wielding a battle-axe in the left hand, should boost the survival probability of individuals with the quaint handedness.

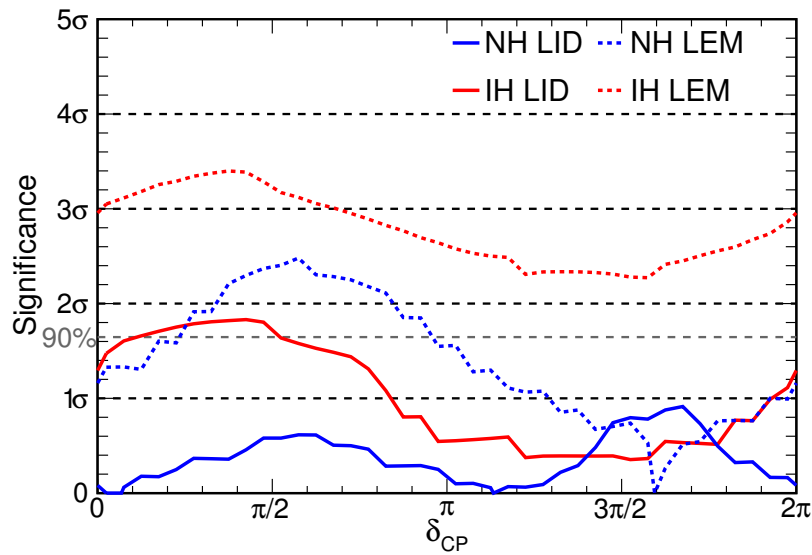


Figure 2.7 – Significance of the difference between the selected and predicted number of events as a function of δ and the mass hierarchy (designated by NH or IH). The disagreement with the observed data is shown in solid lines for the primary Likelihood Identifier (LID), and in dotted lines for the secondary Library Event Matching (LEM) classifier. Figure taken from [61].

Part II

Neutrinos in Double Chooz

Chapter 3

$\overline{\nu}_e$ production at Chooz

As long as particle physicists trade in patience with the safety authorities, nuclear power plants are inexpensive (anti)neutrino sources. All things considered, they are remarkably easier to get by than thermonuclear weapons. Besides, commercial nuclear reactors provide a much steadier flux than the latter or potentially malfunctioning accelerators. For indeed, the money-makers know how willing the folks are to light up their households and blast music at night, and accordingly, try hard to keep the machine roaring. In addition, fuel reloading does shrink the emitted antineutrino rate in a very predictable way. All that being said, the main strength of reactor experiments undeniably lies in the copiousness and purity of this electron antineutrino rate, which the reactors pour isotropically at the near and far detectors.

3.1 Production site

The 757-inhabitant Chooz village – located in northern France, slyly protruding into Belgium, by the Meuse river (cf. Figure 3.1) – has a long history in pioneering nuclear engineering. Indeed, following the American guidelines, Chooz was the target of choice to build the first Pressurised Water Reactor (PWR) in France, in 1967, with a 320 MW generating capacity. Later, the picturesque village welcomed on its banks the first powerful 1450 MW PWR’s, B1 and B2, in 1996 and 1997, respectively.

On top of being a first-class nuclear power site, over the last two decades, Chooz has had tight links with research in particle physics. Before the new generation reactors B1 and B2 were built, the Chooz experiment took advantage of the vast network of tunnels, at the Chooz A site – where the former 320 MW nuclear reactor entered the decommissioning phase in 2001 – to set up its 5 t liquid scintillator antineutrino detector, 100 m underground.

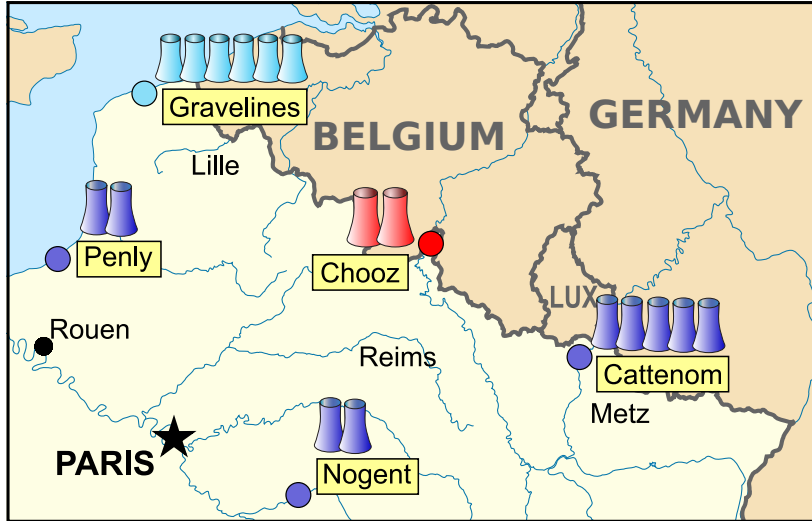


Figure 3.1 – Location of the $\bar{\nu}_e$ factory for the Double Chooz experiment. In red, the two cooling towers of the 2×1450 MW Chooz nuclear power station. For information purposes only, older nuclear reactors are also shown in light blue (900 MW cores) and in purple (1300 MW cores).

3.2 Nuclear fission

3.2.1 Overcoming the Coulomb barrier

Predicting the antineutrino production of a nuclear reactor is no leisurely stroll, for fission itself, is no simple matter.

Nuclear fission is a process in which the nucleus of an atom breaks into lighter nuclei, referred to as "fission fragments". The process can be initiated by a nuclear reaction, such as neutron capture; it may also occur spontaneously, as a usual decay. Fission primarily results from the competition between the nuclear binding force, which increases roughly in proportion to A , the mass number, and the Coulomb repulsion of protons, growing faster as Z^2 , with Z the atomic number. In other words, the higher the ratio Z^2/A , the easier it is for the nucleus to split apart. Naively, if the unstable nucleus ${}_Z^A\text{U}$ were to split into two equal-mass fragments ${}_Z^{A/2}\text{V}$, the characteristic ratio would be divided in two for both fragments, hence the increase in stability, at least with respect to fission. To this end, the fission fragments must first overcome the Coulomb barrier, which inhibits spontaneous fission (see Figure 3.2) in way analogous to α -decay.

The absorption of a relatively small amount of energy, however, forms an intermediate state, which is above the Coulomb barrier, so that fission occurs readily. The absorbed energy may not be too large though, for the cross section decreases with energy: the slower the incoming neutron, the higher the probability to interact with the nucleus. Isotopes with an odd mass but an even atomic number willingly welcome another neutral nucleon, by

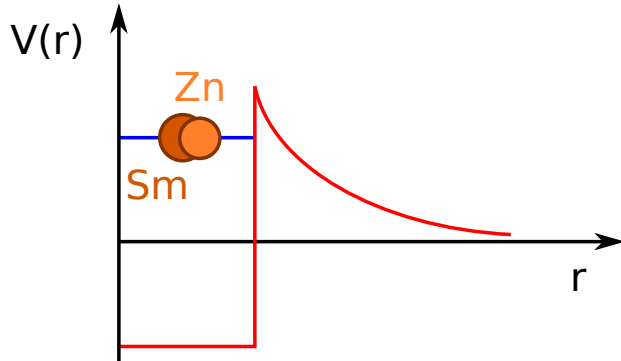
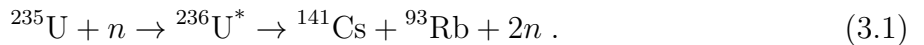


Figure 3.2 – Unless it receives an additional energy from fast neutrons, ^{238}U does not come apart. The two fission fragment candidates, ^{159}Sm and ^{79}Zn , cannot overcome the Coulomb barrier, and are thus trapped by the nuclear potential V , at small r , with r the separation distance between the fission fragments.

means of the pairing force, to which the large fission cross sections of ^{235}U and ^{239}Pu owe much. An example of a fission process, induced by neutron capture, is given in (3.1)



3.2.2 Chain reaction in nuclear reactors

Nuclear reactors indulge in the latter type of mechanism, i.e. neutron capture, and there is many a reaction similar to (3.1) happening in the reactor cores. In accordance, the fission products are not always ^{141}Cs and ^{93}Rb and there actually is a whole distribution of them, which shows two distinct peaks (see Figure 3.3).

Taking into account Figure 3.3, one can show that when uranium is bombarded by a neutron flux in a PWR, its fission is accompanied by the emission of an average of 2.4 neutrons [63]. Out of these 2.4 neutrons, all but one of them is to be lost, either by being absorbed by another nucleus which cannot undergo fission, or by leaving the reactor core. If each fission is accompanied by the effective release of exactly one neutron, the process is self-sustaining, considering that uranium fission is induced by one neutron, as exemplified by (3.1). If too few neutrons are lost, the fission is explosive. If too many are absorbed or spill out, the reaction is just a wet firecracker.

Inasmuch as the fission cross-sections decrease with energy, maintaining a self-sustaining chain reaction implies lowering the energy of the released neutrons. To this end, the nuclear fuel is placed in a neutron moderator. Ideally, out of all choices, the moderator should have a mass closest to $A = 1$ (so that each collision adequately slows the neutrons) while meagrely capturing neutrons. In PWR's, a pressure of 155 bar [63] ensures that ordinary water, the moderator, remains liquid well above its atmospheric boiling point, thereby retaining its capacity to slow neutrons down and transfer the heat from the reactor cores to electrical